

000 001 002 003 004 005 006 007 008 009 010 011 012 013 014 015 016 017 018 019 020 021 022 023 024 025 026 027 028 029 030 031 032 033 034 035 036 037 038 039 040 041 042 043 044 045 046 047 048 049 050 051 052 053 INSIGHT-O3: EMPOWERING MULTIMODAL FOUNDATION MODELS WITH GENERALIZED VISUAL SEARCH

Anonymous authors

Paper under double-blind review

ABSTRACT

The ability for AI agents to “think with images” requires a sophisticated blend of reasoning and perception. However, current open multimodal agents still largely fall short on the reasoning aspect that are crucial for real-world tasks like analyzing documents with dense charts/diagrams and navigating maps. To address this gap, we first introduce O3-BENCH, a new benchmark designed to evaluate multimodal reasoning with interleaved attention to visual details. O3-BENCH features challenging questions that require agents to gather subtle visual information from multiple distinct areas of an image while reasoning upon it. These tasks are highly challenging even for frontier systems like OpenAI o3, which only obtains 42.8% accuracy on O3-BENCH. To tackle these tasks, we propose INSIGHT-O3, a multi-agent framework that divides labor between a visual reasoning agent (vReasoner) and a visual search agent (vSearcher). As a concrete first step towards o3-like open systems, this work focuses on the latter (*i.e.*, vSearcher), for which we introduce the task of generalized visual search—locating relational, fuzzy, or conceptual regions described in free-form language, beyond just simple objects or figures in natural images. We present a multimodal LLM purpose-trained for this task via reinforcement learning. As a plug-and-play agent, our vSearcher empowers frontier multimodal models (as vReasoners) with generalized visual search, significantly improving their performance on a wide range of benchmarks.

1 INTRODUCTION

Thinking with images is an important and very useful skill for multimodal agents (OpenAI, 2025b). The skill rests on two crucial and fundamental cognitive abilities: reasoning and perception. Recent efforts at developing such a skill based on open models mainly focus on the perception component, *e.g.*, searching for a particular object or figure in natural images and then answering a simple visual query about them (Wu & Xie, 2024; Shen et al., 2024; Li et al., 2025; Zhang et al., 2025a; Su et al., 2025a; Zheng et al., 2025; Wang et al., 2025c; Zhu et al., 2025b; Wang et al., 2025a; Lai et al., 2025). While this feature is clearly useful in certain scenarios, it is still far from being able to handle many real-world tasks that require deeper and more abstract reasoning. Typical examples of such tasks include extracting key information from complex reports and navigating through intricate maps to reach a destination. Solving these tasks often require both organized reasoning and focused attention to various visual details scattered across an image.

Currently, the reasoning capability of open multimodal models is still relatively weak in comparison with frontier proprietary models (Yue et al., 2024a; Yuan et al., 2025; Hao et al., 2025). This makes it very difficult to replicate the kind of reasoning-driven image-thinking behavior demonstrated by OpenAI o3 (OpenAI, 2025b). In this work, we take a concrete step towards building such an intelligent system with open models. First, we propose a new multimodal benchmark, O3-BENCH, to help better evaluate the general capability of multimodal models to think with images. Complementary to most of the existing benchmarks which only deal with object attributes and spatial relations in natural images (Wu & Xie, 2024; Wang et al., 2025g; Lai et al., 2025; Wang et al., 2025a), O3-BENCH consists of a set of high-quality, *reasoning-oriented* questions on images of *high information density*. The questions involve real-world tasks such as map navigation and cross-chart/diagram analysis that are highly challenging even for frontier systems like OpenAI o3. Compared with benchmarks like MME-RealWorld (Zhang et al., 2024b), O3-BENCH is significantly harder, requiring the evaluated



Figure 1: A multi-step visual reasoning example of INsIGHT-O3 on O3-BENCH. For clarity, the internal reasoning processes of vReasoner and vSearcher are omitted. More examples can be found in Appendix E.

system to collect detailed visual information from *multiple* distinct image areas while performing *complex, interleaved* reasoning using the information collected in the process.

To make substantive progress on O3-BENCH, we introduce a multi-agent framework, INsIGHT-O3, that comprises a visual reasoning agent (**vReasoner**) and a visual search agent (**vSearcher**). The former is responsible for high-level reasoning and general image understanding, while the latter is to help vReasoner locate specific regions of interest and collect the visual information therein. As such, INsIGHT-O3 reduces the burden of a single agent, allowing us to build an o3-like system via divide-and-conquer. This kind of specialization has been shown to work in prior art (Dayan & Hinton, 1992; Zeng et al., 2023; Shen et al., 2023; Li et al., 2023a; Hong et al., 2023; Castrejon et al., 2024). In this work, we focus on vSearcher and how it should interact with a given vReasoner. Different from current practices (Wu & Xie, 2024; Lai et al., 2025) for natural images and discrete object references, we aim to solve *generalized visual search*, where the input image can be arbitrary, *e.g.*, a map, a poster, or a screenshot; and the referring description may specify a relational, fuzzy, or conceptual region, *e.g.*, "the area to the left of the wooden chair," and "the chart showing the company's revenue in the last decade," rather than a specific object or figure. Such fuzzy descriptions are more in line with how humans reason and direct their attention to a general region of interest.

To address this broader challenge, we present InSight-o3-vS, a vSearcher model specialized in generalized visual search through reinforcement learning. InSight-o3-vS combines multimodal understanding with spatial reasoning to localize regions described in completely free-form language. The

108 name of our model, InSight-o3-vS, reflects its dual role: providing deeper *insight* into multimodal
 109 semantics while bringing the target region *in sight* through precise localization. Our model empow-
 110 ers existing multimodal foundation models (as vReasoners) in a *plug-and-play* fashion, significantly
 111 improving the performance of frontier models across a wide range of benchmarks, *e.g.*, from 38.1%
 112 to 63.4% on O3-BENCH for GPT-5-mini (OpenAI, 2025a), and from 80.1% to 87.6% on V*-Bench
 113 for Gemini-2.5-Flash (Comanici et al., 2025).

114 To summarize, we make the following key contributions in this work:
 115

- 116 • We propose a new benchmark, O3-BENCH, to evaluate complex, reasoning-oriented visual tasks.
 117 This benchmark features challenges like map navigation and cross-chart analysis, which require
 118 collecting information from multiple image areas and performing interleaved reasoning, making
 119 it significantly harder than existing benchmarks.
- 120 • We introduce INSIGHT-O3, a multi-agent framework that divides the task of “thinking with im-
 121 ages” between a high-level reasoning agent (**vReasoner**) and a visual search agent (**vSearcher**).
 122 This divide-and-conquer design greatly simplifies the complex interleaved reasoning, allowing us
 123 to build o3-like systems that surpass OpenAI o3 across a variety of benchmarks.
- 124 • We present InSight-o3-vS, a specialized vSearcher model that excels at *generalized visual search*.
 125 It is designed to be a “plug-and-play” component that empowers existing multimodal foundation
 126 models, demonstrably and significantly improving the performance of frontier systems on a wide
 127 range of benchmarks (*e.g.*, raising GPT-5-mini’s score on O3-BENCH from 38.1% to 63.4%).

128 2 RELATED WORK

131 We provide a brief overview of the most relevant related work in this section. For a more compre-
 132 hensive discussion, please refer to Appendix A.

134 **Multimodal benchmarks.** Classical multimodal benchmarks (Goyal et al., 2017; Saikh et al.,
 135 2022; Liu et al., 2023; Ge et al., 2024) mainly test coarse image-level or salient-attribute recogni-
 136 tion, where modern MLLMs are near-saturated (Bai et al., 2025; Wang et al., 2025e). Recent multi-
 137 modal reasoning benchmark split into (i) cognition-centric STEM benchmarks (Lu et al., 2023;
 138 Yue et al., 2024a;b) that emphasize multi-step/world-knowledge reasoning but use visually simple
 139 images, and (ii) perception-centric datasets (Wu & Xie, 2024; Zhang et al., 2024b; Lai et al., 2025)
 140 that require fine-grained recognition in high-resolution, text-rich scenes yet often limited to single-
 141 region lookups. Motivated by the “think with images” paradigm (OpenAI, 2025b), O3-BENCH
 142 jointly evaluates search/localization and higher-level reasoning on high-information-density charts
 143 and maps, requiring cross-region evidence aggregation via interleaved, multi-hop reasoning.

144 **Multimodal reasoning models.** Reinforcement learning (RL) has long been used to align model
 145 behavior with human preferences (Schulman et al., 2017). DeepSeek-R1 applies group relative
 146 policy optimization (GRPO) (Guo et al., 2025a; Shao et al., 2024b), reliably eliciting planning,
 147 reflection, and long chain-of-thought reasoning under simple rewards. Building on this idea, re-
 148 cent multimodal models (Yang et al., 2025b) adopt GRPO-style training and report strong gains,
 149 while cascaded RL stages (*e.g.*, InternVL3.5 (Wang et al., 2025e), Keye-VL1.5 (Yang et al., 2025a))
 150 further push reasoning, approaching proprietary models. There are also pioneering work utilizing
 151 Python code execution to call various vision tools to solve tasks via divide-and-conquer or to help
 152 with reasoning (Gupta & Kembhavi, 2023; Surís et al., 2023; Ke et al., 2024). Nevertheless, most
 153 multimodal reasoners remain text-centric, overlooking the distinctive demands of visual reasoning.

154 **Visual search models.** Visual search is a core multimodal capability, requiring active region per-
 155 ception for fine-grained understanding. Early methods relied on external detectors or scripted work-
 156 flows to localize regions and triggered tools via instruction tuning, leading to rigid outputs and
 157 typically single-round search (Wu & Xie, 2024). The “think with images” paradigm (OpenAI,
 158 2025b) internalizes zoom/crop operations and has inspired end-to-end search (DeepEyes (Zheng
 159 et al., 2025)), synthetic warm-starts (Pixel-Reasoner (Su et al., 2025a)), and multi-turn RL (Mini-
 160 o3 (Lai et al., 2025)). Nonetheless, most systems still emphasize finding a single region in natural
 161 images, with limited support for multi-hop reasoning. We broaden this scope by decoupling visual
 162 search from visual reasoning and enabling multi-region search on arbitrary images.

162 3 O3-BENCH
163

164 We conceptualize “thinking with images” as an iterative perception-reasoning process. Perception
165 focuses on searching and localizing task-relevant visual details, while reasoning needs to organize
166 these cues into structured facts and performs higher-order inference (*e.g.*, planning, arithmetic, use
167 of world knowledge) to complete the task. These two critical skills should be executed effectively
168 and cooperate tightly to achieve strong performance. Existing benchmarks (Wu & Xie, 2024; Zhang
169 et al., 2024b; Lai et al., 2025) primarily emphasize perception, where their questions hardly re-
170 quire multi-step reasoning and thus induce short reasoning chains. To bridge this gap, we introduce
171 O3-BENCH, a benchmark that jointly assesses high-resolution perception and multi-hop visual rea-
172 soning. O3-BENCH is designed with two principles:

- 173 • **High resolution & high information density.** Images are large, high-resolution, cluttered,
174 and information-dense, making evidence gathering genuinely non-trivial.
- 175 • **Multi-hop solution paths.** Questions require decomposing the goal, retrieving evidence
176 from multiple regions, and composing it via intermediate steps before answering.

178 To instantiate these principles, O3-BENCH comprises two complementary domains: (1) *Composite*
179 *charts*. Each image contains multiple heterogeneous charts (*e.g.*, bar/line/pie/tables). Our crafted
180 questions demand cross-chart retrieval (series, axes, units), lightweight calculations (differences,
181 ratios, aggregates), and consistency checks (scale, legend, time ranges) to derive the final answer. (2)
182 *High-resolution digital maps*. The images typically include a map along with auxiliary components
183 such as legends and building indices. We meticulously design questions that require visual search
184 for targets (*e.g.*, matching symbols, categories, or toponyms) and spatial reasoning about relations
185 and routes (*e.g.*, proximity constraints or shortest paths), conditioned on the provided context.

186 Overall, O3-BENCH comprises 185 images (98 in charts, 87 in maps) and 318 QA samples (136 in
187 chart, 182 in map) in total. The majority of samples fall into the more challenging *map* category,
188 underscoring our prioritization of complex visual perception and multi-hop reasoning. The questions
189 of O3-BENCH are multi-choice questions with six choices and one correct answer. Among the six
190 choices, there are four distractors that appear in the image or look similar to the correct one. We also
191 include an option F as *No Right Choice* if there are no correct options provided. Below, we present
192 the construction process of O3-BENCH. For other details about O3-BENCH, see Appendix B.1.

193 3.1 SOURCE DATA COLLECTION
194

195 **Chart.** The chart images in O3-BENCH are curated from the “Diagram and Table” subset from
196 MME-RealWorld (Zhang et al., 2024b) and the Internet. To ensure high information density, we run
197 a layout detection model, PP-DocLayout_plus-L (Cui et al., 2025), on the candidate images and only
198 keep those with at least 8 detected layouts. As a result, 256 of 2,539 images that contain sufficient
199 number of sub-figures and rich recognizable texts are left.

200 **Map.** We manually collect high-resolution digital maps from the Internet via keyword search. We
201 center on the venue-level maps that require reading the provided legend/index and visually locating
202 entities within the image to answer the question. We exclude all the country-, state-, or city-scale
203 cartography that could be potentially answered with world knowledge. Through this process, we
204 end up with 87 high-density map images spanning the categories over bus routes, campus, park, *etc.*

205 3.2 ANNOTATION PIPELINE
206

208 After the collection and initial filtering process, all images then undergo further manual screening
209 to ensure clarity and completeness of key visual cues (*e.g.*, axes, units and legends). Next, we
210 combine automated machine pre-annotation with human verification and authoring to generate the
211 question-answer (QA) instances. The detailed process of data annotation is presented as follows.

212 **Machine pre-annotation.** To relieve the burden of human annotators and increase the data diver-
213 sity, we first apply a three-step automated data pipeline to generate five questions for each image.
214 (1) *Layout detection*. We divide the high-resolution images into several structured layouts (*e.g.*, ta-
215 bles, charts, legends) using PP-DocLayout_plus-L (Cui et al., 2025). For map images, we review

216 the predictions, correct erroneous regions, and supplement missing areas via manual annotation. (2)
 217 *Information extraction*. For each layout, we prompt Qwen2.5-VL-32B (Bai et al., 2025) to produce
 218 a detailed caption for the layout and extract OCR text from it. In addition, we obtain global context
 219 by generating a caption and extracting the OCR text for the full image. (3) *Automated question*
 220 *synthesis*. For each image, we provide the layout set (with captions and OCR texts) and the global
 221 context to GPT-5 (OpenAI, 2025a) to generate five questions (with answers and explanations) that
 222 compose evidence from the provided layout regions. Note that we do not provide the full image to
 223 GPT-5, compelling it to focus on region-level details and encourages multi-hop composition. More
 224 details about the whole pre-annotation process can be found in Appendix B.2.

225 **Human annotation.** (1) *Filtering and validation*. Annotators start by discarding ill-posed or low-
 226 quality machine-generated QAs (e.g., those with factual inconsistencies, ambiguous prompts, or
 227 spurious multi-hop reasoning). For the retained QAs, annotators verify that the six-option set con-
 228 tains exactly one unambiguous correct answer and confirm that the explanation faithfully, step by
 229 step, justifies the choice. The annotators also ensure that the target layouts are relevant to answering
 230 the question; these layouts are either derived from the explanation or added via manual annotation.
 231 (2) *Human-authored questions*. For information-dense images, machine-generated QAs often con-
 232 tain logical errors, wrong answers, or missed visual details. These QAs are reworked or completely
 233 rewritten by the annotators, adhering to our design principles: requiring fine-grained detail retrieval
 234 and multi-hop reasoning. Each QA includes a detailed explanation to aid verification and have
 235 exactly one unambiguous correct choice among the six.

236 **Difficulty filtering and secondary review.** We evaluate all candidate items with three strong pro-
 237 prietary MLLMs, *i.e.*, GPT-5-mini (OpenAI, 2025a), Gemini-2.5-Flash (Comanici et al., 2025) and
 238 Doubao-Seed-1.6 (Bytedance, 2025), using the same evaluation prompt. We discard any items
 239 solved by all three models to ensure difficulty. Subsequently, independent reviewers (distinct from
 240 the original annotators) conduct cross-verification: a final pass over the QAs and the explanations
 241 to confirm factual correctness, clarity, and formatting consistency. Finally, we confirm with experi-
 242 ments that attention to visual details is vital to good performance on O3-BENCH (see Appendix B.3).
 243

244 4 INSIGHT-O3

245 In the previous section, we introduced O3-BENCH, a meticulously-crafted benchmark that require
 246 problem-solving systems to have both good reasoning and perception capabilities, as well as the
 247 ability to integrate them in a natural, synergetic manner. Recent approaches towards such systems
 248 mostly build upon a single MLLM agent which handles both reasoning and perception workloads
 249 within a single context window (Su et al., 2025a; Zheng et al., 2025; Lai et al., 2025). While this
 250 is reasonable for tasks primarily focusing on either reasoning or perception, the agent may struggle
 251 when the workloads are heavy and intertwined.

252 To address the issue, we propose INSIGHT-O3, a two-agent system that largely decouples the afore-
 253 mentioned burden by a visual reasoning agent (**vReasoner**) and a visual search agent (**vSearcher**).
 254 The former specializes in high-level, abstract reasoning (with some general image understanding
 255 capability), while the latter is mainly responsible for extracting detailed visual information and pre-
 256 senting them to vReasoner. For instance, given a question, vReasoner first decomposes the question
 257 through reasoning, and, if needed, issues relevant image region descriptions to vSearcher; vSearcher
 258 then localizes the requested evidence (with help from tools like image cropping) and returns it for
 259 subsequent rounds until a final answer is produced. This process is illustrated in Figure 2(a). How-
 260 ever, jointly training both agents in a system like INSIGHT-O3 is notoriously difficult—their objec-
 261 tives differ yet are highly interdependent, causing difficulties such as credit assignment across calls,
 262 and non-stationary updates when both policies learn. Additionally, in our case, even the state-of-
 263 the-art open MLLMs, *e.g.*, Qwen2.5-VL-Instruct (Bai et al., 2025), tend to produce overly concise
 264 replies with little thinking process (Lai et al., 2025).

265 To avoid overcomplication, we consider a simpler, more manageable setting in this paper. Specifi-
 266 cally, we delegate higher-order reasoning at training time to a strong external model (*e.g.*, GPT-4o
 267 as vReasoner) and focus on training vSearcher to cooperate with the given vReasoner effectively.
 268 This separation helps simplify optimization and improve data efficiency. Our experiment shows that
 269 a well-trained vSearcher can significantly improve the performance of a wide range of vReasoners

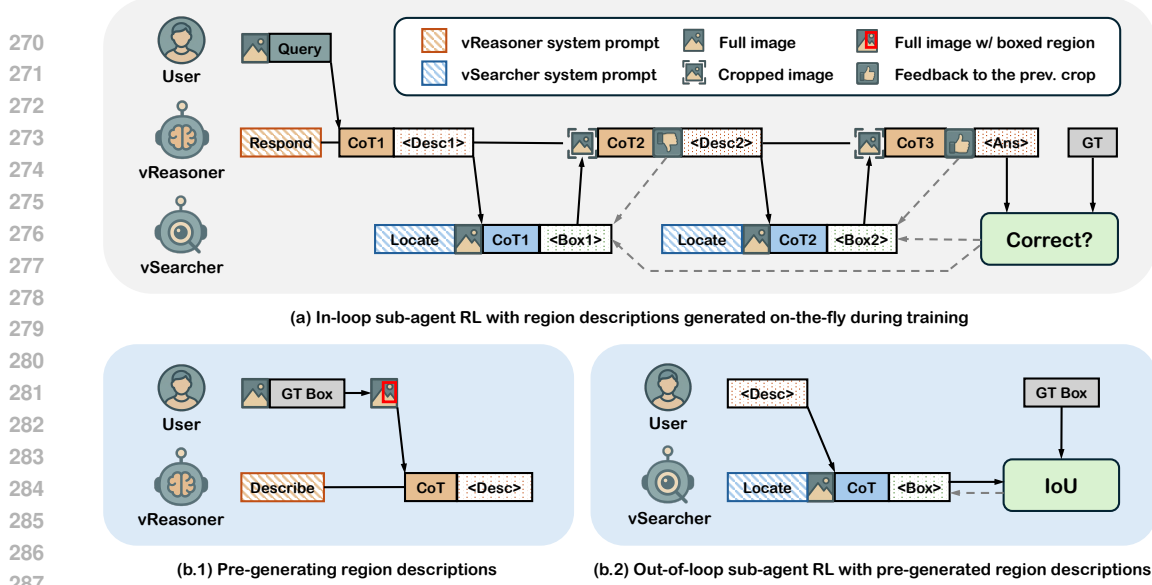


Figure 2: **Training pipeline.** We use a hybrid RL algorithm to train vSearcher. **(a)** In the in-loop component, vReasoner generates visual search tasks on-the-fly during training as it tries to answer a user query. We use vReasoner’s feedback and final answer correctness as supervision (denoted by dashed arrows) for vSearcher. **(b)** In the out-of-loop component, we use pre-generated descriptions with ground-truth bounding boxes, allowing us to train vSearcher efficiently via IoU supervision.

as a plug-and-play callable agent. Furthermore, the resulting system may help synthesize multi-turn supervised-finetuning (SFT) traces with interleaved reasoning and visual search, paving the way for a larger, potentially unified model. While prior works (Su et al., 2025a; Jiang et al., 2025a) have explored role-playing to construct similar SFT traces, the data quality is often not very high as the role-playing agents are only loosely coordinated. In this respect, our approach helps strengthen this coordination with reinforcement learning (RL), as detailed next.

4.1 TRAINING ALGORITHM

We propose a hybrid sub-agent RL algorithm that consists of an *in-loop* component and an *out-of-loop* component to train vSearcher (see Figure 2). In the out-of-loop component, we pre-generate region descriptions with predefined bounding boxes, allowing us to train vSearcher very efficiently via direct IoU supervision. In the in-loop component, we use real descriptions generated on-the-fly during training by vReasoner. Compared with pre-generated tasks, these dynamically generated tasks are more aligned in nature with the tasks that vSearcher will see during inference time.

Reward design. For the out-of-loop RL, we use the following reward function for vSearcher:

$$r = \mathbb{I}[n_{\text{tool}} > 0] \cdot (\lambda_{\text{format}} \cdot r_{\text{format}} + \lambda_{\text{IoU}} \cdot r_{\text{IoU}}), \quad (1)$$

where n_{tool} is the number of tool calls made by vSearcher, $r_{\text{format}} \in \{0, 1\}$ is the format reward, and $r_{\text{IoU}} \in (0, 1)$ is the IoU reward (λ_{format} and λ_{IoU} are weighting coefficients for the rewards). In Eq.(1), the IoU reward r_{IoU} encourages vSearcher to propose an accurate region that matches the description. In addition, we encourage vSearcher to use image cropping¹ at least once to verify that the returned region matches the given region description. For every predicted box b and the ground-truth box b^* , we define the IoU reward as $r_{\text{IoU}} = \max\{0, \text{IoU}(b, b^*) - \alpha\}/(1 - \alpha)$ where $\alpha \in (0, 1)$ controls the reward threshold. Boxes with an IoU less than α are not rewarded.

For the in-loop RL component, we replace the IoU reward r_{IoU} in Eq.(1) with a pseudo IoU reward $\hat{r}_{\text{IoU}} \in \{0, 1\}$. We obtain \hat{r}_{IoU} by asking vReasoner to rate each vSearcher’s prediction, with the rating criterion being whether the prediction is relevant to the assigned task and can help vReasoner

¹For simplicity, we only allow vSearcher to use the most essential image cropping tool. Our framework, however, does not impose such a constraint. It is easy to incorporate other kinds of tools for vSearcher to use.

324 answer the user query. The rating $s \in \{0, 1\}$ is a binary score indicating if the prediction is helpful.
 325 However, as this rating is not always reliable (vReasoner may sometimes make mistakes), we further
 326 incorporate outcome supervision as a safeguard. Let $c \in \{0, 1\}$ stand for whether the final answer
 327 of vReasoner is correct. The pseudo IoU reward is defined as $\hat{r}_{\text{IoU}} = \mathbb{I}[s = c = 1]$.
 328

329 **Advantage estimation.** We follow GRPO (Shao et al., 2024b) to estimate the advantages for the
 330 out-of-loop RL component. As for the in-loop component, we normalize the rewards with respect to
 331 the *global* mean and standard deviation instead of the *group* mean and standard deviation since the
 332 concept of “group” no longer exists for the dynamically generated tasks. Formally, the advantage
 333 of an output token o_t at time step t is computed as $\hat{A}_t = [r - \text{mean}(\mathbf{r})]/\text{std}(\mathbf{r})$, where for the
 334 out-of-loop component, $\mathbf{r} = \{r_i\}_{i=1}^G$ with G being the group size; and for the in-loop component,
 335 $\mathbf{r} = \{r_i\}_{i=1}^N$ with N being the total number of visual search tasks generated on-the-fly by vReasoner.
 336

337 **Objective function.** The objective function we use is based on GRPO (Shao et al., 2024b), with
 338 some modifications (e.g., global advantage estimations) to incorporate the in-loop RL component.
 339 Given a policy model π_θ , the old policy $\pi_{\theta_{\text{old}}}$, and a reference policy π_{ref} , the objective function for
 340 a batch of M vSearcher outputs (including both in-loop and out-of-loop ones) is defined as

$$341 J(\theta) = \frac{1}{M} \sum_{i=1}^M \frac{1}{|o_i|} \sum_{t=1}^{|o_i|} \left\{ \min \left[\gamma_t(\theta) \hat{A}_t, \text{clip}(\gamma_t(\theta), 1 - \epsilon, 1 + \epsilon) \hat{A}_t \right] - \beta \mathbb{D}_{\text{KL}}[\pi_\theta \| \pi_{\text{ref}}] \right\}, \quad (2)$$

344 where $\gamma_t(\theta) = \frac{\pi_\theta(o_{i,t}|q, o_{i,<t})}{\pi_{\theta_{\text{old}}}(o_{i,t}|q, o_{i,<t})}$ is the importance ratio of the output token $o_{i,t}$ given a query q and
 345 all previous output tokens $o_{i,<t}$ including tool-response tokens. During training, we mask the loss
 346 for tool-response tokens as they are not generated by the policy model.
 347

348 4.2 TRAINING DATA CONSTRUCTION

350 As high-resolution, information-dense images with good questions are scarce and difficult to col-
 351 lect on a large scale, we construct training data by synthesizing collages (for the in-loop RL) and
 352 generating pseudo visual search targets (for the out-of-loop RL). The source data are mostly from
 353 existing VQA training datasets, which follow a largely different distribution from O3-BENCH and
 354 other evaluation benchmarks we consider in our experiments.

355 **In-loop RL data.** A key criterion for in-loop RL data is that they must be difficult enough to
 356 incentivize visual search; otherwise vReasoner could simply answer on its own and vSearcher would
 357 receive no reward. To raise search difficulty and ensure meaningful credit assignment, we build
 358 image collages by stitching multiple low-to-medium-resolution images into a canvas. We construct
 359 collages from a filtered combination of Visual CoT (Shao et al., 2024a) and the V* training data (Wu
 360 & Xie, 2024), where each item provides a QA pair and a target bounding box. For each collage,
 361 we choose one target image (carrying the QA) and add several filler images as distractors. After
 362 difficulty filtering, we obtain 15,303 hard problems that vReasoner must rely on vSearcher to solve
 363 reliably. For more construction details and visualizations of the data, see Appendix C.1.
 364

365 **Out-of-loop RL data.** We use InfographicVQA (Mathew et al., 2022) as the image source of the
 366 out-of-loop RL data. Most InfographicVQA images have high information density and feature more
 367 organic and diverse layouts than collages. We detect layout components in the source images with
 368 PP-DocLayout_plus-L (Cui et al., 2025). The candidate layout boxes are filtered and further pro-
 369 cessed, resulting in 10,186 high-quality layout boxes. We then use GPT-5-nano to generate concise,
 370 high-level region descriptions for each box, as illustrated in Figure 2(b.1). Through prompting, we
 371 make GPT-5-nano mimic the style it would use when invoking vSearcher in the in-loop setting. This
 372 process yields a set of (*image, region description, bbox*) which enables the out-of-loop RL. More
 373 construction details and visualizations are provided in the Appendix C.2.
 374

375 5 EXPERIMENT

376 In our main experiments, we train Qwen2.5-VL-7B-Instruct (Bai et al., 2025) as vSearcher un-
 377 der GPT-5-mini-2025-08-07 (OpenAI, 2025a) as vReasoner for balanced efficiency and reasoning

Table 1: **Performance comparison with frontier models/systems.** All models/systems are evaluated under their default configurations unless specified otherwise. Performance of open models are mostly cited from the literature (Wu & Xie, 2024; Zheng et al., 2025; Wang et al., 2025a; Lai et al., 2025). Other results are averaged over 3 trials, except for MME-RW_{Lite} (single-trial). Small-size numbers indicate performance gaps between vReasoners with and without access to vSearchers.

Model/System	V*-Bench	HR-Bench _{4K}	Tree-Bench	VProbe _{Hard}	MME-RW _{Lite}	O3-Bench	Average
LLaVA-OV-7B	70.9	62.0	37.3	13.4	48.5	-	-
InternVL3-8B	-	-	38.8	-	-	-	-
Qwen2.5-VL-7B	75.5	68.2	37.0	23.9	46.7	29.9	46.9
Qwen3-VL-8B	86.4	78.9	48.3	31.6	53.0	45.6	57.3
Pixel Reasoner	86.3	74.0	28.8	28.8	-	-	-
DeepEyes	83.3	73.2	37.5	35.1	-	29.6	-
Mini-o3	88.2	77.5	-	48.0	-	28.4	-
OpenAI o3	76.4	74.3	52.3	23.6	55.2	42.8	54.1
GPT-4o	68.6	65.1	47.4	26.4	51.2	29.9	48.1
+ Qwen2.5-VL-7B	75.2 <small>+6.6</small>	69.7 <small>+4.6</small>	45.9 <small>-1.6</small>	15.4 <small>-11.0</small>	44.6 <small>-6.6</small>	33.8 <small>+3.9</small>	47.4 <small>-0.7</small>
+ InSight-o3-vS	80.4 <small>+11.8</small>	76.2 <small>+11.1</small>	49.5 <small>+2.1</small>	25.5 <small>-1.1</small>	50.1 <small>-1.1</small>	41.9 <small>+12.0</small>	53.9 <small>+5.8</small>
GPT-5-nano	64.0	60.6	45.4	21.7	47.7	28.9	44.7
+ Qwen2.5-VL-7B	70.1 <small>+6.1</small>	67.3 <small>+6.7</small>	45.7 <small>+0.3</small>	18.2 <small>-3.5</small>	44.9 <small>-2.8</small>	29.4 <small>+0.5</small>	45.9 <small>+1.2</small>
+ InSight-o3-vS	75.1 <small>+11.1</small>	72.3 <small>+11.7</small>	47.7 <small>+2.3</small>	31.4 <small>+9.7</small>	48.4 <small>+0.7</small>	34.8 <small>+5.9</small>	51.0 <small>+6.3</small>
GPT-5-mini	73.8	72.0	54.6	26.4	56.1	38.1	53.5
+ Qwen2.5-VL-7B	80.6 <small>+6.8</small>	83.2 <small>+11.2</small>	53.1 <small>-1.5</small>	37.7 <small>+11.3</small>	58.1 <small>+2.0</small>	52.3 <small>+14.2</small>	56.4 <small>+2.9</small>
+ InSight-o3-vS	86.9 <small>+13.1</small>	86.7 <small>+14.7</small>	54.1 <small>-0.5</small>	41.2 <small>+14.6</small>	59.0 <small>+2.9</small>	63.4 <small>+25.3</small>	65.2 <small>+11.7</small>
+ InSight-o3-vS [†]	86.2 <small>+12.4</small>	85.7 <small>+13.7</small>	55.0 <small>+0.4</small>	39.6 <small>+13.2</small>	58.4 <small>+2.3</small>	64.0 <small>+25.9</small>	64.8 <small>+11.3</small>
Gemini-2.5-Flash [#]	72.8	75.0	48.9	17.9	55.6	57.2	54.6
+ Qwen2.5-VL-7B	76.3 <small>+3.5</small>	76.7 <small>+1.7</small>	51.3 <small>+2.4</small>	16.7 <small>-1.2</small>	50.9 <small>-4.7</small>	58.2 <small>+1.0</small>	55.0 <small>+0.4</small>
+ InSight-o3-vS	80.8 <small>+8.0</small>	80.2 <small>+5.2</small>	52.1 <small>+3.2</small>	19.8 <small>+1.9</small>	55.1 <small>-0.5</small>	65.4 <small>+8.2</small>	58.9 <small>+4.3</small>
+ InSight-o3-vS [†]	85.5 <small>+12.7</small>	82.7 <small>+7.7</small>	52.6 <small>+3.7</small>	26.4 <small>+8.5</small>	56.1 <small>+0.5</small>	65.7 <small>+8.5</small>	61.5 <small>+6.9</small>
Gemini-2.5-Flash	80.1	83.5	49.9	39.6	56.5	60.7	61.7
+ Qwen2.5-VL-7B	80.9 <small>+0.8</small>	79.0 <small>-4.5</small>	49.1 <small>+0.8</small>	31.4 <small>-8.2</small>	52.0 <small>-4.5</small>	61.6 <small>+0.9</small>	59.0 <small>-2.7</small>
+ InSight-o3-vS	87.6 <small>+7.5</small>	82.3 <small>-1.2</small>	50.1 <small>+0.2</small>	36.2 <small>-3.4</small>	56.3 <small>-0.2</small>	67.0 <small>+6.3</small>	63.3 <small>+1.6</small>
+ InSight-o3-vS [†]	88.3 <small>+8.2</small>	83.0 <small>-0.5</small>	53.6 <small>+3.7</small>	38.3 <small>-1.3</small>	56.4 <small>-0.1</small>	67.4 <small>+6.7</small>	64.5 <small>+2.8</small>

[†] Trained with Gemini-2.5-Flash as vReasoner.

[#] Image-size constraint tightened to 1280×1280px, same as the maximum supported size for GPT models.

capability. The resulting vSearcher, named InSight-o3-vS, is evaluated under various vReasoners including Gemini-2.5-Flash (Comanici et al., 2025). For comparison, we evaluate these vReasoners normally as standalone models as well (and with the untrained Qwen2.5-VL-7B-Instruct being the vSearcher). We use the default configuration for proprietary models/systems (per official API) except from setting image detail to `high`². More implementation details can be found in Appendix D.

Evaluation datasets. We evaluate a range of open and proprietary models/systems on the following benchmarks: (1) Natural-image benchmarks: V*-Bench (Wu & Xie, 2024), Tree-Bench (Wang et al., 2025a), and VisualProbe-Hard (Lai et al., 2025). (2) Mixed benchmarks: HR-Bench (Wang et al., 2025f) and MME-RealWorld (Zhang et al., 2024b). For efficient evaluation, we use the lite version of MME-RealWorld, which has 1,919 questions, still much heavier than the other benchmarks. (3) Our O3-BENCH. More information about the benchmarks can be found in Appendix J.

5.1 MAIN RESULTS

Cross-domain performance improvement for frontier models. As shown in Table 1, INSIGHT-O3 significantly improves the performance of frontier models such as GPT-5-mini and Gemini-2.5-Flash on most benchmarks. On average, the performance of GPT-5-mini has improved by 22%. In particular, the accuracy of GPT-5-mini on O3-BENCH has nearly doubled (from 38.1% to 63.4%) with the help of our vSearcher (InSight-o3-vS). Meanwhile, INSIGHT-O3 also significantly outperforms their pre-RL counterparts, *i.e.*, vReasoner + Qwen2.5-VL-7B, across all the benchmarks. The results suggest that InSight-o3-vS is able to generalize *out-of-distribution* across various domains since its training data distribution is distinct from the evaluation data distributions. To gain more insight on how INSIGHT-O3 improves the baselines, see Appendix F for a comparative analysis.

²When image detail is set to `high`, OpenAI scales down oversize images to roughly 1280×1280px, as per OpenAI API (<https://platform.openai.com/docs/guides/images-vision#calculating-costs>). This is the maximum supported image resolution for GPT models. Gemini-2.5-Flash API does not impose such a strict constraint, so we use a much larger, 3500×3500px budget that is ample for the purpose.

432 Table 2: **Performance of Gemini-2.5-Flash (+ InSight-o3-vS[†]) under different maximum train-
 433 ing/test image resolutions.** All results are averaged over 3 trials, except for MME-RW_{Lite} (which
 434 is based on a single trial). Small-size numbers indicate performance gaps between settings with and
 435 without vSearcher. [†] Trained with Gemini-2.5-Flash as vReasoner.

Train res.	Test res.	V*-Bench	HR-Bench _{4K}	Tree-Bench	VProbe _{Hard}	MME-RW _{Lite}	O3-Bench	Average
-	1280 ²	72.8	75.0	48.9	17.9	55.6	57.2	54.6
1280 ²	1280 ²	85.5 <small>+12.7</small>	82.7 <small>+7.7</small>	52.6 <small>+3.7</small>	26.4 <small>+8.5</small>	56.1 <small>+0.5</small>	65.7 <small>+8.5</small>	61.5 <small>+6.9</small>
3500 ²	1280 ²	85.3 <small>+12.5</small>	81.3 <small>+6.3</small>	53.1 <small>+4.2</small>	22.6 <small>+4.7</small>	55.1 <small>-0.5</small>	66.9 <small>+9.7</small>	60.7 <small>+6.1</small>
-	3500 ²	80.1	83.5	49.9	39.6	56.5	60.7	61.7
1280 ²	3500 ²	87.8 <small>+7.7</small>	84.3 <small>+0.8</small>	52.1 <small>+2.2</small>	39.6 <small>+0.0</small>	56.4 <small>-0.1</small>	67.5 <small>+6.8</small>	64.6 <small>+2.9</small>
3500 ²	3500 ²	88.3 <small>+8.2</small>	83.0 <small>-0.5</small>	53.6 <small>+3.7</small>	38.3 <small>-1.3</small>	56.4 <small>-0.1</small>	67.4 <small>+6.7</small>	64.5 <small>+2.8</small>

443 Table 3: **Ablation study on reward design and ad-
 444 vantage estimation.** All results are averaged over 3 tri-
 445 als. Small-size numbers indicate performance changes
 446 w.r.t. the proposed setting.

Setting	V*-B.	VP _{Hard}	O3-B.	Avg.
Proposed	86.9	41.2	63.4	63.8
w/o tool cond.	86.4 <small>-0.5</small>	39.3 <small>-1.9</small>	62.6 <small>-0.8</small>	62.8 <small>-1.0</small>
w/o feedback	86.5 <small>-0.4</small>	37.1 <small>-4.1</small>	61.4 <small>-2.0</small>	61.7 <small>-2.1</small>
w/o outcome	86.9 <small>+0.0</small>	38.7 <small>-2.5</small>	63.3 <small>-0.1</small>	63.0 <small>-0.8</small>
w/o GN	87.3 <small>+0.4</small>	36.8 <small>-4.4</small>	60.9 <small>-2.5</small>	61.7 <small>-2.1</small>

447 Table 4: **Sensitivity analysis w.r.t.**
448 max. input resolution of vSearcher.
 449 “#vSearch” is the number of vSearcher
 450 calls made by vReasoner per QA.

Max. pixels	V*-B.	O3-B.	#vSearch
0.8M	85.3	61.5	2.77
1.6M	86.7	63.2	2.60
3.2M	89.4	63.2	2.65
6.4M	86.4	64.0	2.58
12.8M	86.9	63.4	2.55

451 **Generalization under different vReasoners.** We observe that InSight-o3-vS, which was trained
 452 as a sub-agent under GPT-5-mini, generalizes under other vReasoner models as well. As shown
 453 in Table 1, InSight-o3-vS improves the performance of a much smaller model, GPT-5-nano, from
 454 21.7% to 31.4% on VisualProbe-Hard, from 28.9% to 34.8% on O3-BENCH, and from 44.7% to
 455 51.0% overall. Under Gemini-2.5-Flash (a different model family), the advantage remains significant,
 456 showing about 6-7% lead over the baselines on V*-Bench and O3-BENCH. **We have also**
 457 **explored training InSight-o3-vS under Gemini-2.5-Flash instead of GPT-5-mini, and observed simi-**
 458 **lar generalization (see “+ InSight-o3-vS[†]” rows in Table 1).** In few cases where InSight-o3-vS fails
 459 to improve the performance of the vReasoner, *e.g.*, GPT-4o and Gemini-2.5-Flash on VisualProbe-
 460 Hard, we see a sharp decrease in performance as we allow these models to call Qwen2.5-VL-7B.
 461 This suggests that these models are relatively weak at tool calling and multi-turn reasoning. In Ap-
 462 pendix G, we present typical failure cases of INSIGHT-O3; we find that even GPT-5-mini (despite
 463 its great performance) still makes a lot of mistakes.

464 **Performance gaps on O3-BENCH.** Interestingly, on O3-BENCH, we observe that Gemini-2.5-
 465 Flash has a huge edge over GPT-5-mini (when they have no access to vSearcher), but on the other
 466 benchmarks, the edge is not so prominent—Gemini-2.5-Flash is even slightly worse than GPT-5-
 467 mini on Tree-Bench. This suggests that O3-BENCH is indeed quite different from the other bench-
 468 marks, and Gemini-2.5-Flash is particularly good at solving the kind of tasks in O3-BENCH on its
 469 own. Notably, with InSight-o3-vS, GPT-5-mini is able to drastically reduce the gap (from 22.6% to
 470 4.0%) with Gemini-2.5-Flash, demonstrating the importance of thinking with images for addressing
 471 O3-BENCH, and also highlighting the effectiveness of our approach.

472 **Effect of input image resolution.** Comparing the results of Gemini-2.5-Flash in Table 1 under
 473 different maximum input image resolutions, we see that a much higher resolution offers clear ad-
 474 vantages. However, the improvement brought by vSearcher is less when vReasoner can see clearer.
 475 In addition, we find that training under one resolution and evaluating under another seems to have
 476 little impact on the performance (see Table 2). Meanwhile, the input image resolution for vSearcher
 477 has less impact. Table 4 shows the performance of GPT-5-mini + InSight-o3-vS under varying
 478 maximum image resolution of InSight-o3-vS during evaluation. From the results, we can see that
 479 InSight-o3-vS is not sensitive to the resolution, maintaining decent performance on V*-Bench and
 480 O3-BENCH even when the maximum image resolution is only 0.8M (25% of that during training).
 481 As the resolution decreases, the average number of vSearcher calls increases. This is reasonable as
 482 low-resolution images often obscure fine details, making it harder for vSearcher to locate the targets.

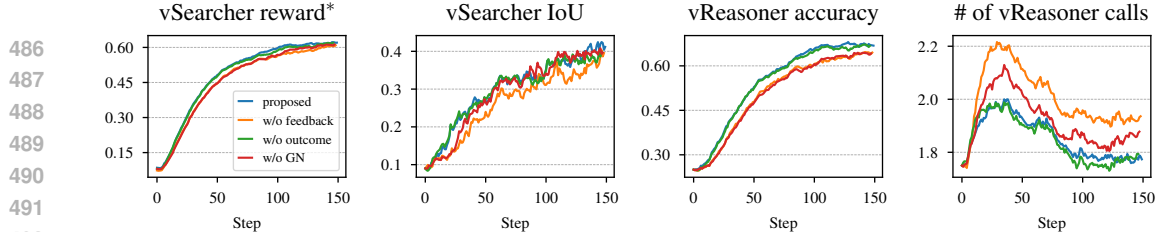


Figure 3: **Training dynamics of InSIGHT-O3.** The rightmost chart, “# of vReasoner calls”, shows the average number of times vReasoner calls vSearcher per QA. * For fair comparison, the reward curves are plotted under the same setting (“w/o feedback”) for all the settings.

5.2 ABLATION STUDY

Hybrid RL training. Table 5 shows the results of ablating the in-loop and the out-of-loop sub-agent RL components. Without the in-loop RL component, training is much faster (81-89% reduction in time per training step) but the final performance is worse on average. Dropping the out-of-loop RL component also hurts the performance; moreover, the training time increases due to more in-loop training. As mentioned in Section 4.2, the two RL components use different training data. The better performance of hybrid RL training can be partly explained by the combined use of the training data. Another contributing factor is the combination of two different sources of supervision (high-level vReasoner feedback and low-level IoU with ground-truth boxes). Overall, combining the two components leads to the best result.

Reward design and advantage estimation. In Table 3, we compare the setting we *proposed* in Section 4.1 on GPT-5-mini + InSIGHT-o3-vS with the following ablated variants: “*w/o tool*” drops the tool condition in the reward function; “*w/o feedback*” removes vReasoner feedback, only using outcome supervision for pseudo IoU reward; “*w/o outcome*” is the opposite of “*w/o feedback*”; and “*w/o GN*” drops the global normalization for advantage estimation. The originally proposed setting outperforms all the variants with a small average lead on the three benchmarks. The training dynamics under these settings are shown in Figure 3. As vSearcher learns to better locate the regions described by vReasoner, we observe that both the out-of-loop localization IoU and the in-loop vReasoner accuracy improve. The non-monotonic “# of vReasoner calls” shows two RL phases of InSIGHT-O3: vSearcher first learns to obey the formatting instructions, and then learns to localize more accurately (so vReasoner could solve the same problem with less vSearcher calls).

Although we encourage vSearcher to use the image-cropping tool, we find the average tool call count often ends up close to 1. There are two underlying reasons for this behavior. First, as mentioned by Zheng et al. (2025); Lai et al. (2025), Qwen2.5-VL-Instruct is often reluctant to call the tool, and does not seem to know how to use the tool properly. Second, vReasoner usually describe a rough region that is not very hard for vSearcher to locate, so the tool has little utility for vSearcher.

6 CONCLUSION

In this work, we introduced O3-BENCH, a high-information-density benchmark that jointly evaluates visual localization and multi-hop reasoning. To advance the research on this challenging benchmark, we proposed InSIGHT-O3, a multi-agent framework that decomposes the “think with images” workflow into high-level reasoning (vReasoner) and visual search (vSearcher). We focus on the training of vSearcher via reinforcement learning to seamlessly cooperate with vReasoner. The specialized InSIGHT-o3-vS can be used as a “plug-and-play” component for existing multimodal foundation models and helps significantly improve the performance of frontier models.

Table 5: **Ablation study on hybrid RL training.** “I.” and “O.” stand for the in-loop and out-of-loop RL components, respectively. “T/step” is the average time per training step. All results are averaged over 3 trials. Small-size numbers indicate performance changes w.r.t. the untrained baselines.

	I.	O.	V* - B.	VP _{Hard}	O3-B.	T/step
GPT-5-mini			70.1	18.2	29.4	-
	✓		74.9 +4.8	23.9 +5.7	33.2 +3.8	846s
	✓	✓	73.7 +3.6	25.1 +6.9	34.6 +5.2	130s
GPT-5-nano	✓	✓	74.5 +4.4	27.4 +9.2	35.9 +6.5	693s
			80.6	37.7	52.3	-
	✓		86.4 +5.8	39.0 +1.3	61.9 +9.6	1223s
GPT-3.5			84.8 +4.2	41.2 +3.5	60.8 +8.5	105s
	✓		86.9 +6.3	41.2 +3.5	63.4 +11.1	941s
	✓	✓				

540 REFERENCES
541

542 Eirikur Agustsson and Radu Timofte. Ntire 2017 challenge on single image super-resolution:
543 Dataset and study. In *Proceedings of the IEEE conference on computer vision and pattern recog-*
544 *nition workshops*, pp. 126–135, 2017. 51

545 Anonymous. Agentorchestra: Orchestrating hierarchical multi-agent intelligence with the tool-
546 environment-agent (TEA) protocol. In *Submitted to The Fourteenth International Confer-*
547 *ence on Learning Representations*, 2025. URL <https://openreview.net/forum?id=YcnKdeI9pp>. under review. 18

548

549 Shuai Bai, Keqin Chen, Xuejing Liu, Jialin Wang, Wenbin Ge, Sibo Song, Kai Dang, Peng Wang,
550 Shijie Wang, Jun Tang, et al. Qwen2. 5-vl technical report. *arXiv preprint arXiv:2502.13923*,
551 2025. 3, 5, 7, 18, 20, 41

552

553 Bytedance. Doubao-Seed-1.6. [https://console.volcengine.com/ark/region:
554 ark+cn-beijing/model/detail?Id=doubao-seed-1-6/](https://console.volcengine.com/ark/region:ark+cn-beijing/model/detail?Id=doubao-seed-1-6/), 2025. 5

555

556 Lluis Castrejon, Thomas Mensink, Howard Zhou, Vittorio Ferrari, Andre Araujo, and Jasper Uij-

557 jlings. Hammr: Hierarchical multimodal react agents for generic vqa. In *NeurIPS 2024 Workshop*
558 *on Compositional Learning: Perspectives, Methods, and Paths Forward*, 2024. 2, 18

559

560 Hardy Chen, Haoqin Tu, Fali Wang, Hui Liu, Xianfeng Tang, Xinya Du, Yuyin Zhou, and Cihang
561 Xie. Sft or rl? an early investigation into training rl-like reasoning large vision-language models.
562 *arXiv preprint arXiv:2504.11468*, 2025a. 18

563

564 Shuang Chen, Yue Guo, Zhaochen Su, Yafu Li, Yulun Wu, Jiacheng Chen, Jiayu Chen, Weijie Wang,
565 Xiaoye Qu, and Yu Cheng. Advancing multimodal reasoning: From optimized cold start to staged
566 reinforcement learning. *arXiv preprint arXiv:2506.04207*, 2025b. 18

567

568 Zihui Cheng, Qiguang Chen, Xiao Xu, Jiaqi Wang, Weiyun Wang, Hao Fei, Yidong Wang, Alex Jin-
569 peng Wang, Zhi Chen, Wanxiang Che, et al. Visual thoughts: A unified perspective of understand-
570 ing multimodal chain-of-thought. *arXiv preprint arXiv:2505.15510*, 2025. 19

571

572 Gheorghe Comanici, Eric Bieber, Mike Schaeckermann, Ice Pasupat, Noveen Sachdeva, Inderjit
573 Dhillon, Marcel Blstein, Ori Ram, Dan Zhang, Evan Rosen, et al. Gemini 2.5: Pushing the
574 frontier with advanced reasoning, multimodality, long context, and next generation agentic capa-
575 bilities. *arXiv preprint arXiv:2507.06261*, 2025. 3, 5, 8, 18

576

577 Cheng Cui, Ting Sun, Manhui Lin, Tingquan Gao, Yubo Zhang, Jiaxuan Liu, Xueqing Wang, Zelun
578 Zhang, Changda Zhou, Hongen Liu, Yue Zhang, Wenyu Lv, Kui Huang, Yichao Zhang, Jing
579 Zhang, Jun Zhang, Yi Liu, Dianhai Yu, and Yanjun Ma. Paddleocr 3.0 technical report, 2025.
580 URL <https://arxiv.org/abs/2507.05595>. 4, 7, 20

581

582 Yufan Dang, Chen Qian, Xueheng Luo, Jingru Fan, Zihao Xie, Ruijie Shi, Weize Chen, Cheng Yang,
583 Xiaoyin Che, Ye Tian, et al. Multi-agent collaboration via evolving orchestration. *arXiv preprint*
584 *arXiv:2505.19591*, 2025. 18

585

586 Peter Dayan and Geoffrey E Hinton. Feudal reinforcement learning. *Advances in neural information*
587 *processing systems*, 5, 1992. 2

588

589 Yihe Deng, Hritik Bansal, Fan Yin, Nanyun Peng, Wei Wang, and Kai-Wei Chang. Openvlthinker:
590 An early exploration to complex vision-language reasoning via iterative self-improvement, 2025.
591 URL <https://arxiv.org/abs/2503.17352>. 18

592

593 Yue Fan, Xuehai He, Diji Yang, Kaizhi Zheng, Ching-Chen Kuo, Yuting Zheng, Sravana Jyothi
594 Narayananaraju, Xinze Guan, and Xin Eric Wang. Grit: Teaching mllms to think with images.
595 *arXiv preprint arXiv:2505.15879*, 2025. 19

596

597 Chaoyou Fu, Peixian Chen, Yunhang Shen, Yulei Qin, Mengdan Zhang, Xu Lin, Zhenyu Qiu, Wei
598 Lin, Jinrui Yang, Xiawu Zheng, et al. Mme: A comprehensive evaluation benchmark for multi-
599 modal large language models. *arXiv preprint arXiv:2306.13394*, 2023. 18

594 Yuying Ge, Sijie Zhao, Jinguo Zhu, Yixiao Ge, Kun Yi, Lin Song, Chen Li, Xiaohan Ding, and Ying
 595 Shan. Seed-x: Multimodal models with unified multi-granularity comprehension and generation.
 596 *arXiv preprint arXiv:2404.14396*, 2024. 3, 18

597

598 Yash Goyal, Tejas Khot, Douglas Summers-Stay, Dhruv Batra, and Devi Parikh. Making the v in vqa
 599 matter: Elevating the role of image understanding in visual question answering. In *Proceedings
 600 of the IEEE conference on computer vision and pattern recognition*, pp. 6904–6913, 2017. 3, 18

601 Daya Guo, Dejian Yang, Haowei Zhang, Junxiao Song, Ruoyu Zhang, Runxin Xu, Qihao Zhu,
 602 Shirong Ma, Peiyi Wang, Xiao Bi, et al. Deepseek-r1: Incentivizing reasoning capability in llms
 603 via reinforcement learning. *arXiv preprint arXiv:2501.12948*, 2025a. 3, 18

604

605 Dong Guo, Faming Wu, Feida Zhu, Fuxing Leng, Guang Shi, Haobin Chen, Haoqi Fan, Jian Wang,
 606 Jianyu Jiang, Jiawei Wang, et al. Seed1. 5-vl technical report. *arXiv preprint arXiv:2505.07062*,
 607 2025b. 18

608 Tanmay Gupta and Aniruddha Kembhavi. Visual programming: Compositional visual reasoning
 609 without training. In *Proceedings of the IEEE/CVF conference on computer vision and pattern
 610 recognition*, pp. 14953–14962, 2023. 3, 19

611

612 Danna Gurari, Qing Li, Abigale J Stangl, Anhong Guo, Chi Lin, Kristen Grauman, Jiebo Luo, and
 613 Jeffrey P Bigham. Vizwiz grand challenge: Answering visual questions from blind people. In
 614 *Proceedings of the IEEE conference on computer vision and pattern recognition*, pp. 3608–3617,
 2018. 18

615

616 Yunzhuo Hao, Jiawei Gu, Huichen Will Wang, Linjie Li, Zhengyuan Yang, Lijuan Wang, and
 617 Yu Cheng. Can mllms reason in multimodality? emma: An enhanced multimodal reasoning
 618 benchmark. In *Forty-second International Conference on Machine Learning*, 2025. 1

619

620 Sirui Hong, Mingchen Zhuge, Jonathan Chen, Xiawu Zheng, Yuheng Cheng, Jinlin Wang, Ceyao
 621 Zhang, Zili Wang, Steven Ka Shing Yau, Zijuan Lin, et al. Metagpt: Meta programming for
 622 a multi-agent collaborative framework. In *The Twelfth International Conference on Learning
 623 Representations*, 2023. 2, 18

624

625 Zhipeng Hou, Junyi Tang, and Yipeng Wang. Halo: Hierarchical autonomous logic-oriented orches-
 tration for multi-agent llm systems. *arXiv preprint arXiv:2505.13516*, 2025. 18

626

627 Jian Hu, Jason Klein Liu, Haotian Xu, and Wei Shen. Reinforce++: An efficient rlhf algorithm with
 628 robustness to both prompt and reward models. *arXiv preprint arXiv:2501.03262*, 2025. 18

629

630 Yushi Hu, Weijia Shi, Xingyu Fu, Dan Roth, Mari Ostendorf, Luke Zettlemoyer, Noah A Smith, and
 631 Ranjay Krishna. Visual sketchpad: Sketching as a visual chain of thought for multimodal lan-
 632 guage models. *Advances in Neural Information Processing Systems*, 37:139348–139379, 2024.
 19

633

634 Wenzuan Huang, Bohan Jia, Zijie Zhai, Shaosheng Cao, Zheyu Ye, Fei Zhao, Zhe Xu, Yao Hu, and
 635 Shaohui Lin. Vision-r1: Incentivizing reasoning capability in multimodal large language models.
 636 *arXiv preprint arXiv:2503.06749*, 2025. 18

637

638 Drew A Hudson and Christopher D Manning. Gqa: A new dataset for real-world visual reasoning
 639 and compositional question answering. In *Proceedings of the IEEE/CVF conference on computer
 640 vision and pattern recognition*, pp. 6700–6709, 2019. 18

641

642 Xinyu Jia, Chuang Zhu, Minzhen Li, Wenqi Tang, and Wenli Zhou. Llivip: A visible-infrared
 643 paired dataset for low-light vision. In *Proceedings of the IEEE/CVF international conference on
 644 computer vision*, pp. 3496–3504, 2021. 51

645

646 Chaoya Jiang, Yongrui Heng, Wei Ye, Han Yang, Haiyang Xu, Ming Yan, Ji Zhang, Fei Huang, and
 647 Shikun Zhang. Vlm-r3: Region recognition, reasoning, and refinement for enhanced multimodal
 648 chain-of-thought. *arXiv preprint arXiv:2505.16192*, 2025a. 6, 19

649

650 Qing Jiang, Xingyu Chen, Zhaoyang Zeng, Junzhi Yu, and Lei Zhang. Rex-thinker: Grounded
 651 object referring via chain-of-thought reasoning. *arXiv preprint arXiv:2506.04034*, 2025b. 19

648 Fucai Ke, Zhixi Cai, Simindokht Jahangard, Weiqing Wang, Pari Delir Haghighi, and Hamid
 649 Rezatofighi. Hydra: A hyper agent for dynamic compositional visual reasoning. In *European*
 650 *Conference on Computer Vision*, pp. 132–149. Springer, 2024. 3, 19

651 Alexander Kirillov, Eric Mintun, Nikhila Ravi, Hanzi Mao, Chloe Rolland, Laura Gustafson, Tete
 652 Xiao, Spencer Whitehead, Alexander C Berg, Wan-Yen Lo, et al. Segment anything. In *Pro-*
 653 *ceedings of the IEEE/CVF international conference on computer vision*, pp. 4015–4026, 2023.
 654 50

655 Xin Lai, Junyi Li, Wei Li, Tao Liu, Tianjian Li, and Hengshuang Zhao. Mini-o3: Scaling up
 656 reasoning patterns and interaction turns for visual search. *arXiv preprint arXiv:2509.07969*, 2025.
 657 1, 2, 3, 4, 5, 8, 10, 18, 19, 50

658 Geng Li, Jinglin Xu, Yunzhen Zhao, and Yuxin Peng. Dyfo: A training-free dynamic focus visual
 659 search for enhancing lmms in fine-grained visual understanding. In *Proceedings of the Computer*
 660 *Vision and Pattern Recognition Conference*, pp. 9098–9108, 2025. 1, 19

661 Guohao Li, Hasan Hammoud, Hani Itani, Dmitrii Khizbulin, and Bernard Ghanem. Camel: Com-
 662 municative agents for “mind” exploration of large language model society. *Advances in Neural*
 663 *Information Processing Systems*, 36:51991–52008, 2023a. 2, 18

664 Kaican Li, Kai Chen, Haoyu Wang, Lanqing Hong, Chaoqiang Ye, Jianhua Han, Yukuai Chen, Wei
 665 Zhang, Chunjing Xu, Dit-Yan Yeung, et al. Coda: A real-world road corner case dataset for
 666 object detection in autonomous driving. In *European conference on computer vision*, pp. 406–
 667 423. Springer, 2022. 51

668 Yifan Li, Yifan Du, Kun Zhou, Jinpeng Wang, Wayne Xin Zhao, and Ji-Rong Wen. Evaluating
 669 object hallucination in large vision-language models. *arXiv preprint arXiv:2305.10355*, 2023b.
 670 18

671 Jiaying Liu, Dong Liu, Wenhan Yang, Sifeng Xia, Xiaoshuai Zhang, and Yuanying Dai. A com-
 672 pre-
 673 hensive benchmark for single image compression artifact reduction. *IEEE Transactions on image*
 674 *processing*, 29:7845–7860, 2020. 51

675 Yuan Liu, Haodong Duan, Yuanhan Zhang, Bo Li, Songyang Zhang, Wangbo Zhao, Yike Yuan,
 676 Jiaqi Wang, Conghui He, Ziwei Liu, et al. Mmbench: Is your multi-modal model an all-around
 677 player? *arXiv preprint arXiv:2307.06281*, 2023. 3, 18

678 Ziyu Liu, Yuhang Zang, Yushan Zou, Zijian Liang, Xiaoyi Dong, Yuhang Cao, Haodong
 679 Duan, Dahua Lin, and Jiaqi Wang. Visual agentic reinforcement fine-tuning. *arXiv preprint*
 680 *arXiv:2505.14246*, 2025. 19

681 Pan Lu, Hritik Bansal, Tony Xia, Jiacheng Liu, Chunyuan Li, Hannaneh Hajishirzi, Hao Cheng, Kai-
 682 Wei Chang, Michel Galley, and Jianfeng Gao. Mathvista: Evaluating mathematical reasoning of
 683 foundation models in visual contexts. *arXiv preprint arXiv:2310.02255*, 2023. 3, 18, 52

684 Minesh Mathew, Viraj Bagal, Rubèn Tito, Dimosthenis Karatzas, Ernest Valveny, and CV Jawahar.
 685 Infographicvqa. In *Proceedings of the IEEE/CVF Winter Conference on Applications of Computer*
 686 *Vision*, pp. 1697–1706, 2022. 7

687 Fanqing Meng, Lingxiao Du, Zongkai Liu, Zhixiang Zhou, Quanfeng Lu, Daocheng Fu, Tiancheng
 688 Han, Botian Shi, Wenhui Wang, Junjun He, et al. Mm-eureka: Exploring the frontiers of multi-
 689 modal reasoning with rule-based reinforcement learning. *arXiv preprint arXiv:2503.07365*, 2025.
 690 18

691 Minheng Ni, Zhengyuan Yang, Linjie Li, Chung-Ching Lin, Kevin Lin, Wangmeng Zuo, and Li-
 692 juan Wang. Point-rft: Improving multimodal reasoning with visually grounded reinforcement
 693 finetuning. *arXiv preprint arXiv:2505.19702*, 2025. 19

694 OpenAI. OpenAI GPT-5. <https://openai.com/index/introducing-gpt-5/>, 2025a.
 695 3, 5, 7, 18, 20, 31, 42, 44, 50

696 OpenAI. OpenAI o3 and o4-mini. [https://openai.com/index/introducing-o3-](https://openai.com/index/introducing-o3-and-o4-mini/)
 697 [and-o4-mini/](https://openai.com/index/introducing-o3-and-o4-mini/), 2025b. 1, 3, 18, 19

702 Yi Peng, Peiyu Wang, Xiaokun Wang, Yichen Wei, Jiangbo Pei, Weijie Qiu, Ai Jian, Yunzhuo Hao,
 703 Jiachun Pan, Tianyidan Xie, et al. Skywork r1v: Pioneering multimodal reasoning with chain-of-
 704 thought. *arXiv preprint arXiv:2504.05599*, 2025. 18

705

706 Ji Qi, Ming Ding, Weihan Wang, Yushi Bai, Qingsong Lv, Wenyi Hong, Bin Xu, Lei Hou, Juanzi
 707 Li, Yuxiao Dong, et al. Cogcom: Train large vision-language models diving into details through
 708 chain of manipulations. *arXiv preprint arXiv:2402.04236*, 2024. 19

709

710 Yusu Qian, Hanrong Ye, Jean-Philippe Fauconnier, Peter Grasch, Yinfei Yang, and Zhe Gan. Mia-
 711 bench: Towards better instruction following evaluation of multimodal llms, 2024. URL <https://arxiv.org/abs/2407.01509>. 52

712

713 Rafael Rafailov, Archit Sharma, Eric Mitchell, Christopher D Manning, Stefano Ermon, and Chelsea
 714 Finn. Direct preference optimization: Your language model is secretly a reward model. *Advances
 715 in neural information processing systems*, 36:53728–53741, 2023. 18

716

717 Christopher Rawles, Sarah Clinckemaillie, Yifan Chang, Jonathan Waltz, Gabrielle Lau, Marybeth
 718 Fair, Alice Li, William Bishop, Wei Li, Folawiyo Campbell-Ajala, Daniel Toyama, Robert Berry,
 719 Divya Tyamagundlu, Timothy Lillicrap, and Oriana Riva. Androidworld: A dynamic benchmark-
 720 ing environment for autonomous agents, 2024. URL <https://arxiv.org/abs/2405.14573>. 52

721

722 Enna Sachdeva, Nakul Agarwal, Suhas Chundi, Sean Roelofs, Jiachen Li, Mykel Kochenderfer,
 723 Chiho Choi, and Behzad Dariush. Rank2tell: A multimodal driving dataset for joint importance
 724 ranking and reasoning. In *Proceedings of the IEEE/CVF winter conference on applications of
 725 computer vision*, pp. 7513–7522, 2024. 51

726

727 Tanik Saikh, Tirthankar Ghosal, Amish Mittal, Asif Ekbal, and Pushpak Bhattacharyya. Scienceqa:
 728 A novel resource for question answering on scholarly articles. *International Journal on Digital
 729 Libraries*, 23(3):289–301, 2022. 3, 18

730

731 John Schulman, Filip Wolski, Prafulla Dhariwal, Alec Radford, and Oleg Klimov. Proximal policy
 732 optimization algorithms. *arXiv preprint arXiv:1707.06347*, 2017. 3, 18

733

734 Hao Shao, Shengju Qian, Han Xiao, Guanglu Song, Zhuofan Zong, Letian Wang, Yu Liu, and Hong-
 735 sheng Li. Visual cot: Unleashing chain-of-thought reasoning in multi-modal language models.
 736 *CoRR*, 2024a. 7, 19, 27

737

738 Zhihong Shao, Peiyi Wang, Qihao Zhu, Runxin Xu, Junxiao Song, Xiao Bi, Haowei Zhang,
 739 Mingchuan Zhang, YK Li, Yang Wu, et al. Deepseekmath: Pushing the limits of mathematical
 740 reasoning in open language models. *arXiv preprint arXiv:2402.03300*, 2024b. 3, 7, 18

741

742 Haozhan Shen, Kangjia Zhao, Tiancheng Zhao, Ruochen Xu, Zilun Zhang, Mingwei Zhu, and Jian-
 743 wei Yin. Zoomeye: Enhancing multimodal llms with human-like zooming capabilities through
 744 tree-based image exploration. *arXiv preprint arXiv:2411.16044*, 2024. 1

745

746 Haozhan Shen, Peng Liu, Jingcheng Li, Chunxin Fang, Yibo Ma, Jiajia Liao, Qiaoli Shen, Zilun
 747 Zhang, Kangjia Zhao, Qianqian Zhang, et al. Vlm-r1: A stable and generalizable r1-style large
 748 vision-language model. *arXiv preprint arXiv:2504.07615*, 2025a. 18

749

750 Wei Shen, Jiangbo Pei, Yi Peng, Xuchen Song, Yang Liu, Jian Peng, Haofeng Sun, Yunzhuo
 751 Hao, Peiyu Wang, Jianhao Zhang, et al. Skywork-r1v3 technical report. *arXiv preprint
 752 arXiv:2507.06167*, 2025b. 18

753

754 Yongliang Shen, Kaitao Song, Xu Tan, Dongsheng Li, Weiming Lu, and Yueting Zhuang. Hugging-
 755 gpt: Solving ai tasks with chatgpt and its friends in hugging face. *Advances in Neural Information
 756 Processing Systems*, 36:38154–38180, 2023. 2, 18, 19

757

758 Guangming Sheng, Chi Zhang, Zilingfeng Ye, Xibin Wu, Wang Zhang, Ru Zhang, Yanghua Peng,
 759 Haibin Lin, and Chuan Wu. Hybridflow: A flexible and efficient rlhf framework. *arXiv preprint
 760 arXiv: 2409.19256*, 2024. 31

756 Alex Su, Haozhe Wang, Weiming Ren, Fangzhen Lin, and Wenhui Chen. Pixel reasoner: In-
 757 centivizing pixel-space reasoning with curiosity-driven reinforcement learning. *arXiv preprint*
 758 *arXiv:2505.15966*, 2025a. 1, 3, 5, 6, 19

759

760 Zhaochen Su, Linjie Li, Mingyang Song, Yunzhuo Hao, Zhengyuan Yang, Jun Zhang, Guanjie
 761 Chen, Jiawei Gu, Juntao Li, Xiaoye Qu, et al. Openthinkimg: Learning to think with images via
 762 visual tool reinforcement learning. *arXiv preprint arXiv:2505.08617*, 2025b. 19

763

764 Xian Sun, Peijin Wang, Zhiyuan Yan, Feng Xu, Ruiping Wang, Wenhui Diao, Jin Chen, Jihao Li,
 765 Yingchao Feng, Tao Xu, et al. Fair1m: A benchmark dataset for fine-grained object recognition in
 766 high-resolution remote sensing imagery. *ISPRS Journal of Photogrammetry and Remote Sensing*,
 767 184:116–130, 2022. 51

768

769 Dídac Surís, Sachit Menon, and Carl Vondrick. Vipergrpt: Visual inference via python execution
 770 for reasoning. In *Proceedings of the IEEE/CVF international conference on computer vision*, pp.
 771 11888–11898, 2023. 3, 19

772

773 Gemini Robotics Team, Saminda Abeyruwan, Joshua Ainslie, Jean-Baptiste Alayrac, Montser-
 774 rat Gonzalez Arenas, Travis Armstrong, Ashwin Balakrishna, Robert Baruch, Maria Bauza,
 775 Michiel Blokzijl, et al. Gemini robotics: Bringing ai into the physical world. *arXiv preprint*
 776 *arXiv:2503.20020*, 2025a. 52

777

778 Kimi Team, Angang Du, Bohong Yin, Bowei Xing, Bowen Qu, Bowen Wang, Cheng Chen,
 779 Chenlin Zhang, Chenzhuang Du, Chu Wei, et al. Kimi-vl technical report. *arXiv preprint*
 780 *arXiv:2504.07491*, 2025b. 18

781

782 Kwai Keye Team, Biao Yang, Bin Wen, Changyi Liu, Chenglong Chu, Chengru Song, Chongling
 783 Rao, Chuan Yi, Da Li, Dunju Zang, et al. Kwai keye-vl technical report. *arXiv preprint*
 784 *arXiv:2507.01949*, 2025c. 18

785

786 V Team, Wenyi Hong, Wenmeng Yu, Xiaotao Gu, Guo Wang, Guobing Gan, Haomiao Tang, Jiale
 787 Cheng, Ji Qi, Junhui Ji, Lihang Pan, Shuaiqi Duan, Weihan Wang, Yan Wang, Yean Cheng,
 788 Zehai He, Zhe Su, Zhen Yang, Ziyang Pan, Aohan Zeng, Baoxu Wang, Bin Chen, Boyan Shi,
 789 Changyu Pang, Chenhui Zhang, Da Yin, Fan Yang, Guoqing Chen, Jiazheng Xu, Jiale Zhu, Jiali
 790 Chen, Jing Chen, Jinhao Chen, Jinghao Lin, Jinjiang Wang, Junjie Chen, Leqi Lei, Letian Gong,
 791 Leyi Pan, Mingdao Liu, Mingde Xu, Mingzhi Zhang, Qinkai Zheng, Sheng Yang, Shi Zhong,
 792 Shiyu Huang, Shuyuan Zhao, Siyan Xue, Shangqin Tu, Shengbiao Meng, Tianshu Zhang, Tianwei
 793 Luo, Tianxiang Hao, Tianyu Tong, Wenkai Li, Wei Jia, Xiao Liu, Xiaohan Zhang, Xin Lyu,
 794 Xinyue Fan, Xuancheng Huang, Yanling Wang, Yadong Xue, Yanfeng Wang, Yanzi Wang, Yifan
 795 An, Yifan Du, Yiming Shi, Yiheng Huang, Yilin Niu, Yuan Wang, Yuanchang Yue, Yuchen Li,
 796 Yutao Zhang, Yuting Wang, Yu Wang, Yuxuan Zhang, Zhao Xue, Zhenyu Hou, Zhengxiao Du,
 797 Zihan Wang, Peng Zhang, Debing Liu, Bin Xu, Juanzi Li, Minlie Huang, Yuxiao Dong, and Jie
 798 Tang. Glm-4.5v and glm-4.1v-thinking: Towards versatile multimodal reasoning with scalable
 799 reinforcement learning, 2025d. URL <https://arxiv.org/abs/2507.01006>. 18

800

801 Haochen Wang, Xiangtai Li, Zilong Huang, Anran Wang, Jiacong Wang, Tao Zhang, Jiani Zheng,
 802 Sule Bai, Zijian Kang, Jiashi Feng, et al. Traceable evidence enhanced visual grounded reasoning:
 803 Evaluation and methodology. *arXiv preprint arXiv:2507.07999*, 2025a. 1, 8, 18, 50

804

805 Haozhe Wang, Chao Qu, Zuming Huang, Wei Chu, Fangzhen Lin, and Wenhui Chen. Vi-
 806 rethinker: Incentivizing self-reflection of vision-language models with reinforcement learning.
 807 *arXiv preprint arXiv:2504.08837*, 2025b. 18

808

809 Jiacong Wang, Zijian Kang, Haochen Wang, Haiyong Jiang, Jiawen Li, Bohong Wu, Ya Wang,
 810 Jiao Ran, Xiao Liang, Chao Feng, et al. Vgr: Visual grounded reasoning. *arXiv preprint*
 811 *arXiv:2506.11991*, 2025c. 1, 19

812

813 Ke Wang, Junting Pan, Weikang Shi, Zimu Lu, Houxing Ren, Aojun Zhou, Mingjie Zhan, and Hong-
 814 sheng Li. Measuring multimodal mathematical reasoning with math-vision dataset. *Advances in*
 815 *Neural Information Processing Systems*, 37:95095–95169, 2024. 18, 52

810 Peiyu Wang, Yichen Wei, Yi Peng, Xiaokun Wang, Weijie Qiu, Wei Shen, Tianyidan Xie, Jiangbo
 811 Pei, Jianhao Zhang, Yunzhuo Hao, et al. Skywork r1v2: Multimodal hybrid reinforcement learn-
 812 ing for reasoning. *arXiv preprint arXiv:2504.16656*, 2025d. 18

813

814 Weiyun Wang, Zhangwei Gao, Lixin Gu, Hengjun Pu, Long Cui, Xingguang Wei, Zhaoyang Liu,
 815 Linglin Jing, Shenglong Ye, Jie Shao, et al. Internvl3. 5: Advancing open-source multimodal
 816 models in versatility, reasoning, and efficiency. *arXiv preprint arXiv:2508.18265*, 2025e. 3, 18

817

818 Wenbin Wang, Liang Ding, Minyan Zeng, Xiabin Zhou, Li Shen, Yong Luo, Wei Yu, and Dacheng
 819 Tao. Divide, conquer and combine: A training-free framework for high-resolution image percep-
 820 tion in multimodal large language models. In *Proceedings of the AAAI Conference on Artificial
 821 Intelligence*, volume 39, pp. 7907–7915, 2025f. 8, 50

822

823 Wenbin Wang, Liang Ding, Minyan Zeng, Xiabin Zhou, Li Shen, Yong Luo, Wei Yu, and Dacheng
 824 Tao. Divide, conquer and combine: A training-free framework for high-resolution image percep-
 825 tion in multimodal large language models. In *Proceedings of the AAAI Conference on Artificial
 826 Intelligence*, volume 39, pp. 7907–7915, 2025g. 1, 18

827

828 Ye Wang, Qianglong Chen, Zejun Li, Siyuan Wang, Shijie Guo, Zhirui Zhang, and Zhongyu Wei.
 829 Simple o3: Towards interleaved vision-language reasoning. *arXiv preprint arXiv:2508.12109*,
 830 2025h. 19

831

832 Yana Wei, Liang Zhao, Jianjian Sun, Kangheng Lin, Jisheng Yin, Jingcheng Hu, Yinmin Zhang,
 833 En Yu, Haoran Lv, Zejia Weng, et al. Open vision reasoner: Transferring linguistic cognitive
 834 behavior for visual reasoning. *arXiv preprint arXiv:2507.05255*, 2025. 18

835

836 Penghao Wu and Saining Xie. V*: Guided visual search as a core mechanism in multimodal llms.
 837 In *Proceedings of the IEEE/CVF Conference on Computer Vision and Pattern Recognition*, pp.
 838 13084–13094, 2024. 1, 2, 3, 4, 7, 8, 18, 19, 27, 50

839

840 Qingyun Wu, Gagan Bansal, Jieyu Zhang, Yiran Wu, Beibin Li, Erkang Zhu, Li Jiang, Xiaoyun
 841 Zhang, Shaokun Zhang, Jiale Liu, et al. Autogen: Enabling next-gen llm applications via multi-
 842 agent conversations. In *First Conference on Language Modeling*, 2024. 18

843

844 LLM-Core-Team Xiaomi. Mimo-vl technical report, 2025. URL <https://arxiv.org/abs/2506.03569>. 18

845

846 Tianbao Xie, Danyang Zhang, Jixuan Chen, Xiaochuan Li, Siheng Zhao, Ruisheng Cao, Toh Jing
 847 Hua, Zhoujun Cheng, Dongchan Shin, Fangyu Lei, Yitao Liu, Yiheng Xu, Shuyan Zhou, Silvio
 848 Savarese, Caiming Xiong, Victor Zhong, and Tao Yu. Osworld: Benchmarking multimodal agents
 849 for open-ended tasks in real computer environments, 2024. 52

850

851 Biao Yang, Bin Wen, Boyang Ding, Changyi Liu, Chenglong Chu, Chengru Song, Chongling
 852 Rao, Chuan Yi, Da Li, Dunju Zang, et al. Kwai keye-vl 1.5 technical report. *arXiv preprint
 853 arXiv:2509.01563*, 2025a. 3, 18

854

855 Qinzhong Yang, Dongdong Chen, Zhentao Tan, Qiankun Liu, Qi Chu, Jianmin Bao, Lu Yuan, Gang
 856 Hua, and Nenghai Yu. Hq-50k: A large-scale, high-quality dataset for image restoration. *arXiv
 857 preprint arXiv:2306.05390*, 2023. 51

858

859 Yi Yang, Xiaoxuan He, Hongkun Pan, Xiyan Jiang, Yan Deng, Xingtao Yang, Haoyu Lu, Dacheng
 860 Yin, Fengyun Rao, Minfeng Zhu, et al. R1-onevision: Advancing generalized multimodal rea-
 861 soning through cross-modal formalization. *arXiv preprint arXiv:2503.10615*, 2025b. 3, 18

862

863 Jiakang Yuan, Tianshuo Peng, Yilei Jiang, Yiting Lu, Renrui Zhang, Kaituo Feng, Chaoyou Fu,
 864 Tao Chen, Lei Bai, Bo Zhang, et al. Mme-reasoning: A comprehensive benchmark for logical
 865 reasoning in mllms. *arXiv preprint arXiv:2505.21327*, 2025. 1

866

867 Xiang Yue, Yuansheng Ni, Kai Zhang, Tianyu Zheng, Ruoqi Liu, Ge Zhang, Samuel Stevens,
 868 Dongfu Jiang, Weiming Ren, Yuxuan Sun, et al. Mmmu: A massive multi-discipline multi-
 869 modal understanding and reasoning benchmark for expert agi. In *Proceedings of the IEEE/CVF
 870 Conference on Computer Vision and Pattern Recognition*, pp. 9556–9567, 2024a. 1, 3, 18

864 Xiang Yue, Tianyu Zheng, Yuansheng Ni, Yubo Wang, Kai Zhang, Shengbang Tong, Yuxuan Sun,
 865 Botao Yu, Ge Zhang, Huan Sun, et al. Mmmu-pro: A more robust multi-discipline multimodal
 866 understanding benchmark. *arXiv preprint arXiv:2409.02813*, 2024b. 3, 18
 867

868 Andy Zeng, Maria Attarian, Krzysztof Marcin Choromanski, Adrian Wong, Stefan Welker, Federico
 869 Tombari, Aveek Purohit, Michael S Ryoo, Vikas Sindhwani, Johnny Lee, et al. Socratic models:
 870 Composing zero-shot multimodal reasoning with language. In *The Eleventh International Con-*
 871 *ference on Learning Representations*, 2023. 2, 18

872 Kaihao Zhang, Dongxu Li, Wenhan Luo, Wenqi Ren, Björn Stenger, Wei Liu, Hongdong Li, and
 873 Ming-Hsuan Yang. Benchmarking ultra-high-definition image super-resolution. In *Proceedings*
 874 *of the IEEE/CVF international conference on computer vision*, pp. 14769–14778, 2021. 51

875 Renrui Zhang, Dongzhi Jiang, Yichi Zhang, Haokun Lin, Ziyu Guo, Pengshuo Qiu, Aojun Zhou,
 876 Pan Lu, Kai-Wei Chang, Yu Qiao, et al. Mathverse: Does your multi-modal ILM truly see the
 877 diagrams in visual math problems? In *European Conference on Computer Vision*, pp. 169–186.
 878 Springer, 2024a. 18
 879

880 Xintong Zhang, Zhi Gao, Bofei Zhang, Pengxiang Li, Xiaowen Zhang, Yang Liu, Tao Yuan, Yuwei
 881 Wu, Yunde Jia, Song-Chun Zhu, et al. Chain-of-focus: Adaptive visual search and zooming for
 882 multimodal reasoning via RL. *arXiv preprint arXiv:2505.15436*, 2025a. 1, 19

883 Yi-Fan Zhang, Huanyu Zhang, Haochen Tian, Chaoyou Fu, Shuangqing Zhang, Junfei Wu, Feng
 884 Li, Kun Wang, Qingsong Wen, Zhang Zhang, et al. Mme-realworld: Could your multimodal
 885 ILM challenge high-resolution real-world scenarios that are difficult for humans? *arXiv preprint*
 886 *arXiv:2408.13257*, 2024b. 1, 3, 4, 8, 18, 51

887 Yi-Fan Zhang, Xingyu Lu, Shukang Yin, Chaoyou Fu, Wei Chen, Xiao Hu, Bin Wen, Kaiyu
 888 Jiang, Changyi Liu, Tianke Zhang, et al. Thyme: Think beyond images. *arXiv preprint*
 889 *arXiv:2508.11630*, 2025b. 19
 890

891 Shitian Zhao, Haoquan Zhang, Shaoheng Lin, Ming Li, Qilong Wu, Kaipeng Zhang, and Chen Wei.
 892 Pyvision: Agentic vision with dynamic tooling. *arXiv preprint arXiv:2507.07998*, 2025. 19
 893

894 Ziwei Zheng, Michael Yang, Jack Hong, Chenxiao Zhao, Guohai Xu, Le Yang, Chao Shen, and
 895 Xing Yu. Deepeyes: Incentivizing “thinking with images” via reinforcement learning. *arXiv*
 896 *preprint arXiv:2505.14362*, 2025. 1, 3, 5, 8, 10, 19, 48

897 Enshen Zhou, Jingkun An, Cheng Chi, Yi Han, Shanyu Rong, Chi Zhang, Pengwei Wang,
 898 Zhongyuan Wang, Tiejun Huang, Lu Sheng, et al. Roborefer: Towards spatial referring with
 899 reasoning in vision-language models for robotics. *arXiv preprint arXiv:2506.04308*, 2025. 52

900 Jinguo Zhu, Weiyun Wang, Zhe Chen, Zhaoyang Liu, Shenglong Ye, Lixin Gu, Hao Tian, Yuchen
 901 Duan, Weijie Su, Jie Shao, et al. Internvl3: Exploring advanced training and test-time recipes for
 902 open-source multimodal models. *arXiv preprint arXiv:2504.10479*, 2025a. 18
 903

904 Muzhi Zhu, Hao Zhong, Canyu Zhao, Zongze Du, Zheng Huang, Mingyu Liu, Hao Chen, Cheng
 905 Zou, Jingdong Chen, Ming Yang, et al. Active-o3: Empowering multimodal large language
 906 models with active perception via grpo. *arXiv preprint arXiv:2505.21457*, 2025b. 1, 19

907 Pengfei Zhu, Longyin Wen, Dawei Du, Xiao Bian, Heng Fan, Qinghua Hu, and Haibin Ling. De-
 908 tection and tracking meet drones challenge. *IEEE transactions on pattern analysis and machine*
 909 *intelligence*, 44(11):7380–7399, 2021. 51
 910
 911
 912
 913
 914
 915
 916
 917

918 A MORE DISCUSSION ON RELATED WORK
919920 A.1 MULTIMODAL BENCHMARKS
921

922 Classical multimodal benchmarks (Goyal et al., 2017; Hudson & Manning, 2019; Gurari et al.,
923 Saikh et al., 2022; Li et al., 2023b; Fu et al., 2023; Liu et al., 2023; Ge et al., 2024) primarily
924 focus on coarse image-level understanding or target at salient-object attributes, on which current
925 multimodal models (Bai et al., 2025; Wang et al., 2025e; Yang et al., 2025a) show near-saturated
926 performance. With growing attention to multimodal reasoning, more challenging benchmarks have
927 emerged, which could be categorized as two groups. (1) Cognition-centric benchmarks. STEM (sci-
928 ence, technology, engineering, and mathematics) benchmarks (Lu et al., 2023; Wang et al., 2024;
929 Zhang et al., 2024a; Yue et al., 2024a;b) evaluate the model’s multi-step reasoning, integration of
930 world knowledge, and complex calculations to solve scientific problems, whereas the accompany-
931 ing images are generally straightforward to interpret. (2) Perception-centric benchmarks. These
932 benchmarks (Wu & Xie, 2024; Wang et al., 2025g; Zhang et al., 2024b; Lai et al., 2025) require
933 fine-grained perception in high-resolution images and strong OCR recognition on text-rich scenes.
934 Nevertheless, many questions become routine once the model precisely localizes the target region,
935 allowing for single-glance solutions. Though the recent TreeBench (Wang et al., 2025a) evaluates
936 second-order reasoning over object spatial transformations, depth ordering, and *etc*, it still centers
937 on a single region in natural images, leaving cross-region evidence aggregation largely underex-
938 plored. With the emergence of the “think with images” paradigm (OpenAI, 2025b), we argue that a
939 well-designed benchmarks should evaluate the joint perceptual and cognitive skills. Our proposed
940 O3-BENCH fills the research gap by meticulously constructing hard questions on high-information
941 density images (*e.g.*, composite graphs, maps), therefore requiring models to gather information
942 from multiple, spatially distinct regions and to perform complex, interleaved reasoning.

943 A.2 MULTIMODAL REASONING MODELS
944

945 Reinforcement learning (RL) (Schulman et al., 2017; Rafailov et al., 2023; Hu et al., 2025) has long
946 been used to align the response of large language models (LLMs) and multimodal LLMs (MLLMs)
947 with human preferences. Recently, DeepSeek-R1 (Guo et al., 2025a) creatively applied group rel-
948 ative policy optimization (GRPO) (Shao et al., 2024b) to LLMs, estimating the mean and variance
949 of advantages across response groups under a simple reward signal. This strategy reliably elicits
950 behaviors such as planning, thinking, and self-reflection, enabling long chain-of-thought (CoT) rea-
951 soning and moving toward more general-purpose reasoning capabilities. Building on this success,
952 several works (Huang et al., 2025; Yang et al., 2025b; Meng et al., 2025; Chen et al., 2025a; Wang
953 et al., 2025b; Shen et al., 2025a; Chen et al., 2025b; Deng et al., 2025; Wei et al., 2025; Peng et al.,
954 2025; Wang et al., 2025d; Shen et al., 2025b) explore cold-start initialization and GRPO-based RL
955 training for multimodal models (*e.g.*, Qwen2.5-VL (Bai et al., 2025)) and report substantial gains on
956 science- and math-oriented benchmarks. Concurrently, InternVL3.5 (Zhu et al., 2025a; Wang et al.,
957 2025e) and Keye-VL1.5 (Team et al., 2025c; Yang et al., 2025a) further leverage cascaded, iterative
958 RL stages to push the frontier of reasoning ability, achieving performance competitive with propri-
959 etary models (OpenAI, 2025a; Comanici et al., 2025). Nevertheless, current multimodal reasoning
960 models (Xiaomi, 2025; Team et al., 2025d; Guo et al., 2025b; Team et al., 2025b) still focus on text-
961 centric reasoning, neglecting the distinctive demands of visual reasoning in multimodal scenarios.

962 A.3 HIERARCHICAL AGENT FRAMEWORKS AND TOOL-USING MULTIMODAL AGENTS
963

964 Recent work has shown that hierarchical collaboration among specialized agents can significantly
965 improve performance on complex tasks. Socratic Models (Zeng et al., 2023) and HuggingGPT (Shen
966 et al., 2023) demonstrate early examples of LLM-based orchestration over expert models via lan-
967 guage. More structured frameworks like CAMEL (Li et al., 2023a), MetaGPT (Hong et al., 2023),
968 and HAMMR (Castrejon et al., 2024) explore role-based or modular specialization with coordinated
969 task decomposition. Others, including AutoGen (Wu et al., 2024), HALO (Hou et al., 2025), Pup-
970 peteer (Dang et al., 2025), and AgentOrchestra (Anonymous, 2025), further extend this paradigm
971 with explicit planning hierarchies, adaptive execution, and learned orchestration, consistently out-
972 performing flat-agent baselines across diverse domains.

Recent works have also explored equipping multimodal models with tool-use and programmatic reasoning to tackle complex visual tasks. VisProg (Visual Programming) (Gupta & Kembhavi, 2023) and ViperGPT (Surís et al., 2023) are two pioneering approaches that use large language models to generate and execute code for orchestrating vision modules. Beyond static program generation, other agents use LLMs as high-level controllers. For example, HuggingGPT (Shen et al., 2023) demonstrates an LLM (ChatGPT) orchestrating numerous specialized models (for vision, language, etc.) More recently, HYDRA (Ke et al., 2024) introduces a dynamic multi-stage framework for visual reasoning: it integrates an LLM-based planner and reasoner with a reinforcement learning-based controller that adapts the sequence of operations via feedback loops, yielding more reliable step-by-step reasoning. These tool-augmented systems highlight the power of combining learned vision-language models with external modules or code execution to improve flexibility and compositional reasoning. In contrast, our work (INSIGHT-O3) targets a complementary gap by introducing a dedicated visual search agent that can be invoked by reasoning agents to locate fine-grained, conceptually described regions within images. This specialized capability, absent in prior tool-using frameworks, allows an INSIGHT-O3-enabled system to pinpoint relevant visual details based on free-form descriptions, thereby enhancing multimodal reasoning with more precise visual understanding.

A.4 VISUAL SEARCH MODELS

Visual search is an important functionality in the multimodal domain, requiring the models to perform active perception over regions of interest (RoIs) for fine-grained visual understanding. Early approaches (Wu & Xie, 2024; Shao et al., 2024a; Qi et al., 2024; Hu et al., 2024; Li et al., 2025) rely on external tools or predefined workflows for region localization and use instruction tuning to trigger tool use. These models exhibit rigid output patterns and typically support only a single round of visual search, which limits their effectiveness in complex scenes. Recently, the milestone OpenAI o3 (OpenAI, 2025b) established the “think with images” paradigm, in which image manipulations (e.g., zooming, cropping) are internalized as intrinsic capabilities, enabling image–text interleaved reasoning. The community has rapidly turned the attention to the promising field. DeepEyes (Zheng et al., 2025) exploits the inherent grounding ability of MLLMs and incentivizes visual search via end-to-end reinforcement learning. Pixel-Reasoner (Su et al., 2025a) improves search accuracy by warm-start instruction tuning on synthesized data with error-induced self-correction trajectories. Mini-o3 (Lai et al., 2025) introduces an over-turn masking technique during RL to encourage multi-turn interaction, markedly enhancing reasoning adaptability and diversity. Other lines of work (Zhao et al., 2025; Zhang et al., 2025b; Liu et al., 2025) resort to write codes for executing multiple image manipulations (e.g., cropping, rotation, enhancement), pointing to an open-ended toolkit for visual reasoning. Although effective, recent advanced methods (Zhu et al., 2025b; Fan et al., 2025; Zhang et al., 2025a; Su et al., 2025b; Ni et al., 2025; Cheng et al., 2025; Jiang et al., 2025a;b; Wang et al., 2025c;h) still largely prioritize locating a single region on natural images, which sidelines the model’s capacity for reasoning. This paper broadens the capability scope of visual search models by decoupling visual reasoning and visual search agents, allowing the receiving of any images and searching of multiple distinct regions.

B ADDITIONAL INFORMATION ON O3-BENCH

B.1 BENCHMARK STATISTICS

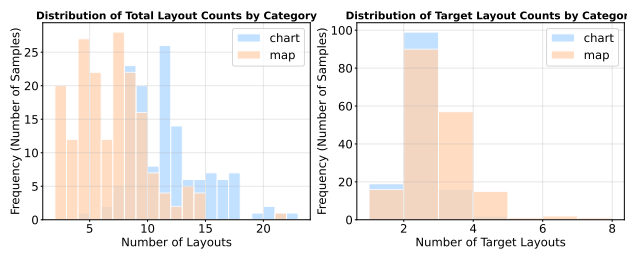


Figure 4: Distribution of layout numbers in O3-BENCH.

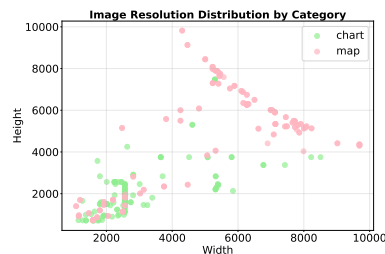


Figure 5: Distribution of resolution.

We summarize the benchmark statistics from following three aspects. **(1) Distribution of layouts.** The benchmark features 8.5 layouts and 2.3 target layouts for each sample on average, indicating high information density and the need for multi-step reasoning. And the layout distribution by category is displayed in Figure 4. It can be seen that chart images typically exhibit a larger set of total layouts, whereas map images require more target layouts for reasoning. **(2) Distribution of resolution.** We collect high-resolution imagery in O3-BENCH. As shown in Figure 5, most images have side lengths in the 2K–4K range, while map images reach up to ~ 10 K pixels on the longer side, yielding high information density. On average, image height and width are 3,967 and 4,602 pixels, respectively. **(3) Distribution of options.** We randomly shuffle options A–E, ensuring an approximately uniform distribution of correct-answer positions. And a small portion (8.2%) of samples use option F (*No Right Choice*) as correct answer, which compels models to aggregate evidence across the entire image and determine that none of the other options is valid.

B.2 DETAILS OF MACHINE PRE-ANNOTATION

(1) *Layout detection.* We first divide the high-resolution images into several structured layouts (*e.g.*, tables, charts, legends). We use PP-DocLayout_plus-L (Cui et al., 2025) to detect layout bounding boxes in the image and construct the set $\mathcal{L} = \{l_i\}_{i=1}^m$, where $l_i \in \mathbb{R}^4$ denotes layout coordinates. For chart images, we directly use the detector outputs. For map images, we review the predictions, correct erroneous regions, and supplement missing areas via manual annotation.

(2) *Information extraction.* For each detected layout l_i in image I , we obtain the cropped image I_{l_i} according to its coordinates. We then prompt Qwen2.5-VL-32B (Bai et al., 2025) to produce a detailed caption c_i and extract OCR text o_i for I_{l_i} , thereby forming the layout triplet $\tau_i = (I_{l_i}, c_i, o_i)$. And then we aggregate all region triplets into $\mathcal{T} = \{\tau_i\}_{i=1}^m$. In addition, we obtain global context by generating a caption and OCR text for the full image, denoted as $\mathcal{G} = (c_g, o_g)$. The prompts we use are provided in Appendix H.1.

(3) *Automated question synthesis.* We provide the layout set \mathcal{T} and the global context \mathcal{G} to GPT-5 (OpenAI, 2025a) and explicitly prompt it to generate five questions that compose evidence from multiple regions. For each question, GPT-5 must produce six options (A–F) with exactly one correct answer, and option F is reserved for *No Right Choice*. It also need to supply a step-by-step explanation that interprets the reasoning chain. It is noted that we do not provide the full image to GPT-5, which compels the model to focus on region-level details and encourages multi-hop composition. The prompts we use are provided in Appendix H.2.

B.3 MORE EXPERIMENTAL RESULTS FOR O3-BENCH

We present additional results for O3-BENCH in this section. Because our annotation pipeline supplies the target layouts most relevant to each question, we can provide these region crops alongside the original full image at test time. We evaluate GPT-5-Mini (OpenAI, 2025a) and Qwen2.5-VL-7B (Bai et al., 2025), with results shown in Table 6. Both models exhibit significant performance gains when given the additional target layouts, underscoring the need for models to actively locate task-critical regions and perform interleaved visual reasoning.

B.4 VISUALIZATION OF O3-BENCH

In Figures 6–11, we present six representative visualizations (four map items and two chart items), showing how O3-BENCH couples high-resolution perception with multi-step reasoning. Each annotation includes: (i) the multiple-choice question and answer; (ii) highlighted target layouts that mark the regions consulted along the solution path; and (iii) a concise, ordered explanation that composes the evidence, which allows readers to verify the answer quickly.

Table 6: Ablation on target layouts in O3-BENCH.

Model	O3-BENCH		
	chart	map	overall
GPT-5-mini	38.2	37.9	38.1
+ target layouts	74.3	53.3	62.3
Qwen2.5-VL-7B	36.0	25.3	29.9
+ target layouts	46.3	28.0	35.9

1080

1081

1082

1083

1084

1085

Annotation**Split:** Map**Q&A:** What is the building opposite the main entrance of the School of Business Postgraduate Annexe?A. MlnT Study; B. Commerce Building; C. Psychology, Darwin House; D. Philosophy, Union St East; E. Pacific Islands Centre; F. None of above**Target Layouts:** **Explanation:** **Step 1.** Locate the School of Business Postgraduate Annexe in the building list , identified as No. 26 at F7. **Step 2.** Find this building at F7 on the East Campus map . **Step 3.** Refer to the Map Legend to confirm that the triangle represents the Main Entrance to the Building. Observe that the main entrance of the School of Business Postgraduate Annexe faces Building No. 27. **Step 4.** Look up Building No. 27 in the building list , identified as the Commerce Building, thus the answer is B.

1094

1095

1096

1097

1098

1099

1100

1101

1102

1103

1104

1105

1106

1107

1108

1109

1110

1111

1112

1113

1114

1115

1116

1117

1118

1119

1120

1121

1122

1123

1124

1125

1126

1127

1128

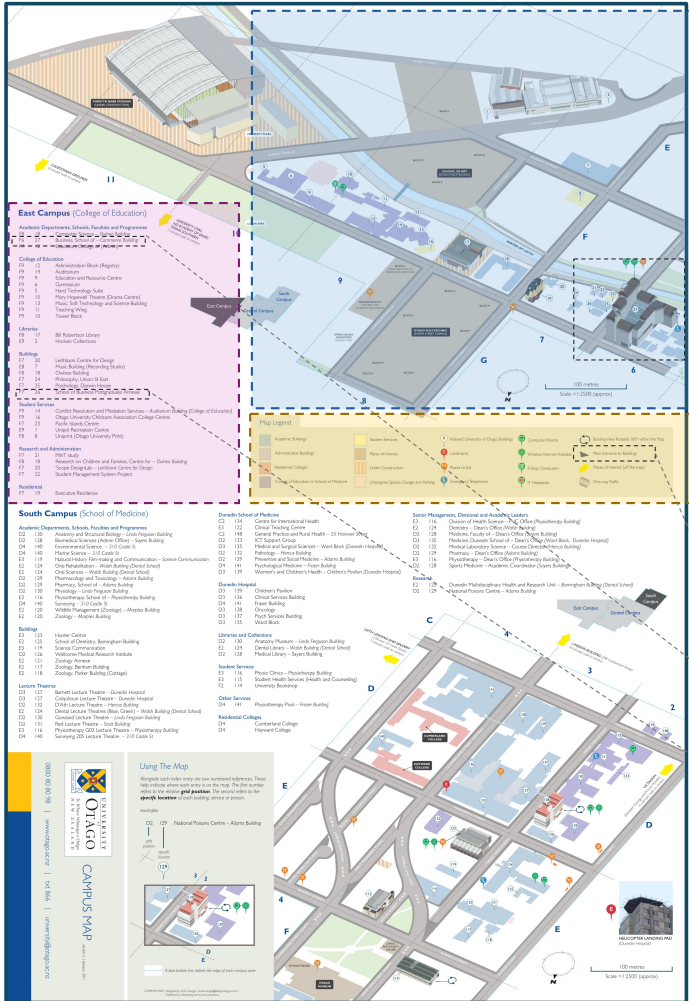
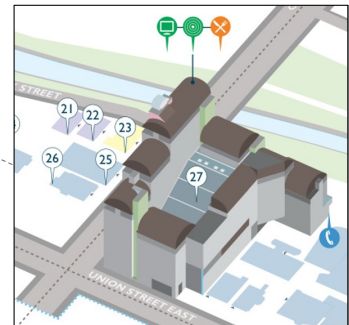
1129

1130

1131

1132

1133

**Closed views of key regions:****Step 3** **Step 2**

Main Entrance to Buildings

Step 4

F6 27 Business, School of – Commerce Building

Step 1

F7 26 School of Business Postgraduate Annexe

1134

1135

1136

1137

Annotation**Split:** Map**Q&A:** Which floor has the Prayer room, and near which zone is it located?

A. 2F, South zone; B. 2F, North zone; C. 3F, North zone; D. 4F, North zone;
E. 4F, West zone; F. None of above

Target Layouts:

Explanation: Step 1. Refer to the Legend to identify the symbol for the Prayer room. Step 2. Use the Floor Guide in the bottom-right corner to find that the Prayer room is located on 2F. Step 3. On the 2F map , locate the Prayer room to the right of the H&M store in the North zone. Select option B accordingly.

**Closed views of key regions:****Step 1** :

Prayer room

Step 3 :**Step 2** :

1182

1183

1184

1185

1186

1187

Figure 7: Example from O3-BENCH (Map-2). Each annotation comprises a six-choice QA and a brief explanation with highlighted target layouts for quick verification; additionally, we also provide step-wise close-ups (outside the annotation) to reveal the evidence chain in large images where fine details may be hard to see.

1188

1189

1190 **Annotation**1191 **Split:** Map1192 **Q&A:** Which restaurant has an ATM located next to it?1193 A. Burger Federation; B. Fulton Street Café; C. Wolfgang Express; D. Goose Island
1194 Beer Company; E. Facades Bar; F. The Bronze Tap1195 **Target Layouts:**   1196 **Explanation:** Step 1. Locate the ATM symbol in PASSENGER SERVICES  Step 2. Match the boarding gate
1197 numbers of the restaurants listed in the options using the restaurant list : Burger Federation (L20),
1198 Fulton Street Cafe (H14), Wolfgang Express (K12), Goose Island Beer Company (L10A), Facades Bar (K15),
1199 The Bronze Tap (K5). Step 3. Compare the gate locations on the terminal map  and identify which gate
1200 has an ATM symbol nearby. Only K5 has an ATM symbol, so the answer is The Bronze Tap, F

1200

1201

1202

1203

1204

1205

1206

1207

1208

1209

1210

1211

1212

1213

1214

1215

1216

1217

1218

1219

1220

1221

1222

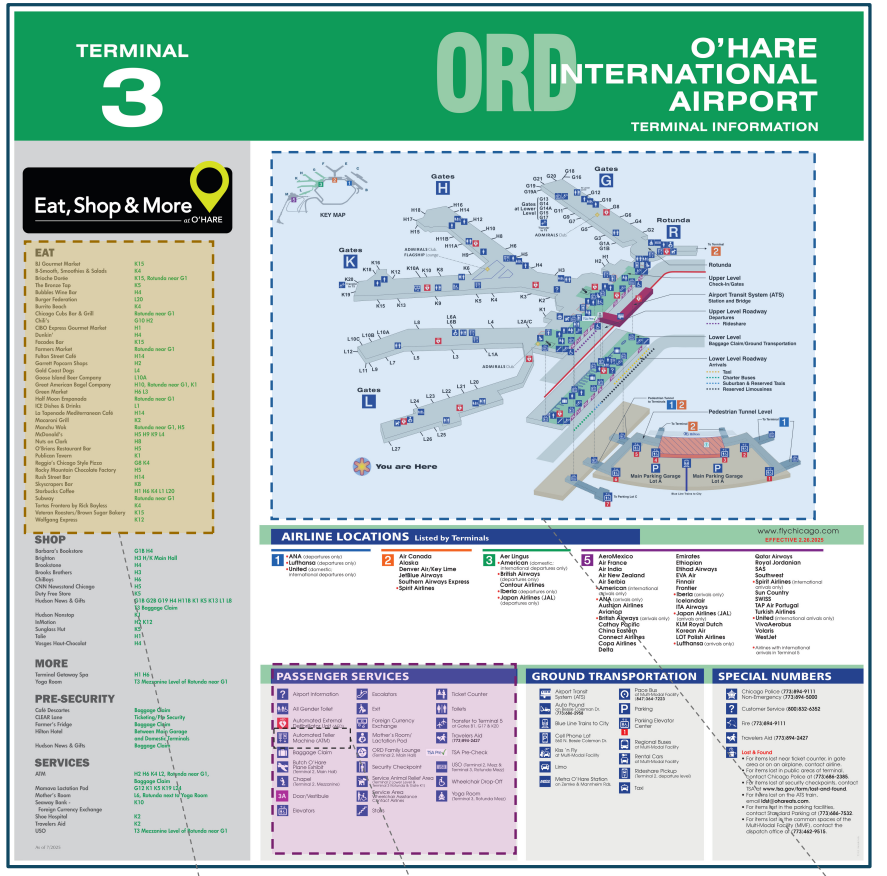
1223

1224

1225

1226

1227



1228

1229



Closed views of key regions:

Step 2 :

Burger Federation	L20
Fulton Street Café	H14
Wolfgang Express	K12
Goose Island Beer Company	L10A
Facades Bar	K15
The Bronze Tap	K5

Step 1 :

1242

1243

1244

1245

1246

Annotation

1247

Split: Map

1248

Q&A: After having lunch at Brookfield Cafe, I want to take a bus to visit Boole Library. Which route should I take?

1250

A. 201; B. 202; C. 205; D. 208; E. 209; F. 216

1251

Target Layouts:

1252

Explanation: **Step 1.** Locate Brookfield Cafe in the Catering list of ; it is building 13 in Grid C7. **Step 2.** Locate Boole Library in ; it is building 11 in Grid F6. **Step 3.** On the map , find that Route 205 bus from College Road below building 13 leads to the vicinity of building 11."

1254



1289

Figure 9: Example from O3-BENCH (Map-4). Each annotation comprises a six-choice QA and a brief explanation with highlighted target layouts for quick verification; additionally, we also provide step-wise close-ups (outside the annotation) to reveal the evidence chain in large images where fine details may be hard to see.

1290

1291

1292

1293

1294

1295

1296

1297

1298

1299

1300

1301

1302

1303

1304

1305

1306

1307

1308

1309

1310

1311

1312

1313

1314

1315

1316

1317

1318

1319

1320

1321

1322

1323

1324

1325

1326

1327

1328

1329

1330

1331

1332

1333

1334

1335

1336

1337

1338

1339

1340

1341

1342

1343

1344

1345

1346

1347

1348

1349

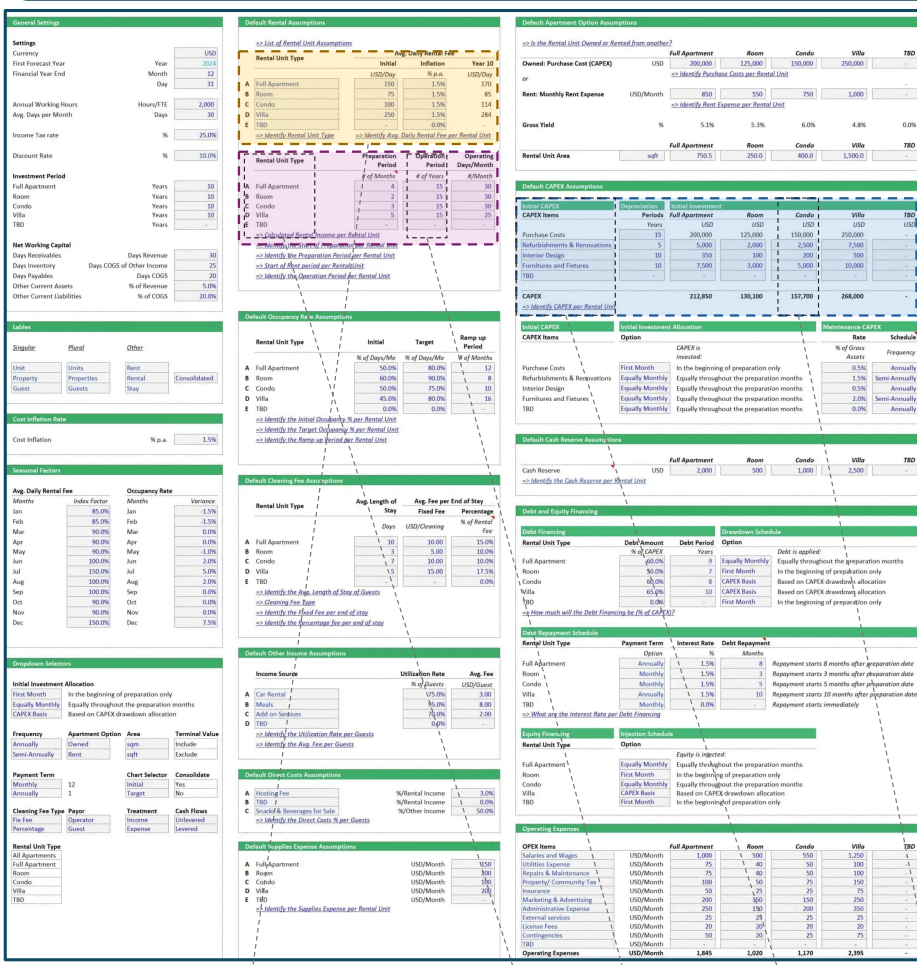
Annotation**Split: Chart**

Q&A: If the Condo unit's Purchase Cost is depreciated evenly over its stated operation period, what percentage does this depreciation amount account for of its Avg. Annual Rental Fee (annualized based on the Year 10 Avg. Daily Rental Fee and 30 days/month)?

A. 35.8%; B. 36.0%; C. 37.5%; D. 38.5%; E. 39.0% F. No right choice

Target Layouts: 

Explanation: Step 1: From , Condo Purchase Costs = 150,000 USD. Step 2: From , depreciation period = 15 years. Therefore, Annual depreciation = 150,000 / 15 = 10,000 USD/year. Step 3: From , Condo Year 10 Avg. Daily Rental Fee = 114 USD/day. Step 4: Annual rental income at Year 10 rate with 30 days/month = 114 * 30 * 12 = 41,040 USD/year. Step 5: Percentage = (10,000 / 41,040) * 100 ≈ 24.37%. Step 6: 24.37% is not listed in options A-E, so the correct choice is F.

 **Closed views of key regions:****Step 3 **:

Rental Unit Type		Avg. Daily Rental Fee		
		Initial	Inflation	Year 10
		USD/Day	% p.a.	USD/Day
A	Full Apartment	150	1.5%	170
B	Room	75	1.5%	85
C	Condo	100	1.5%	114
D	Villa	250	1.5%	284
E	TBD	-	0.0%	-

 Identify Rental Unit Type  Identify Avg. Daily Rental Fee per Rental Unit

Step 2 :

Rental Unit Type	Operation Period	
	# of Years	
A	Full Apartment	15
B	Room	15
C	Condo	15
D	Villa	15
E	TBD	-

Initial CAPEX	CAPEX Items	Condo
Purchase Costs	150,000	USD
Refurbishments & Renovations	2,500	
Interior Design	200	
Furniture and Fixtures	5,000	
TBD	-	

1404
1405**B.5 COMPARISON WITH MME-REALWORLD (CHART)**1406
1407
1408
1409

The chart images of O3-BENCH are from the “Diagram & Table“ subset of MME-RealWorld. The original questions from MME-RealWorld are relatively simple, usually focusing on a single value in a chart, which do not require any kind of multi-hop reasoning. For example, the original question of MME-RealWorld for the chart we show in Figure 10 is:

1410

What is the cost inflation rate in the General Settings section of the General Assumptions table?

1412

In comparison, the new question in O3-BENCH is:

1414
1415
1416
1417

If the Condo unit’s Purchase Cost is depreciated evenly over its stated operation period, what percentage does this depreciation amount account for of its Avg. Annual Rental Fee (annualized based on the Year 10 Avg. Daily Rental Fee and 30 days/month)?

1418
1419
1420

As illustrated in Figure 10, answering this question requires gathering detailed information from *three* different tables and connecting the information through multi-step reasoning and calculations.

1421
1422

Overall, the questions of O3-BENCH (chart) are much more difficult than the MME-RealWorld counterparts. This can also be seen from the following statistics:

1423

- The average accuracy of GPT-5-mini on O3-BENCH (chart) is about 38.2%, whereas on MME-RealWorld (chart), the accuracy is about 82.4%.
- The average number of vSearch steps of InSight-o3 on O3-BENCH (chart) is about 3.1, whereas on MME-RealWorld (chart), the number is about 1.1.
- The average response length of GPT-5-mini vReasoner on O3-BENCH (chart) is about 1942.3 characters, whereas on MME-RealWorld (chart), the average response length is about 730.0 characters.

1431

C TRAINING DATA CONSTRUCTION DETAILS1432
1433
1434
1435**C.1 IN-LOOP RL DATA**1436
1437
1438
1439
1440
1441
1442
1443
1444
1445

Our collage sources come from the training split of Visual CoT (Shao et al., 2024a) and V* (Wu & Xie, 2024). We first filter both datasets by target bounding box size, retaining items with $\text{area(bbox)}/\text{area(image)} < 0.04$. From Visual CoT, we keep all Chart/OCR-centric subsets (dude, cub, textvqa, docvqa, infographicsvqa, sroie, vsr, textcap), and treat the natural-image subsets (flickr30k, gqa, openimages, v7w) together with V* as a separate stream due to lower QA reliability (*e.g.*, weaker question–image alignment and non-unique answers). To ensure stable RL rewards, we filter this stream with an MLLM check using Qwen2.5-VL-7B and GPT-5-nano under a deterministic prompt. An item is retained only if both models return correct answer; otherwise it is discarded, including ambiguous or poorly aligned cases. After this pipeline, we retain $\sim 100K$ items as the source pool \mathcal{D} for collage synthesis.

1446
1447
1448
1449
1450
1451
1452
1453
1454
1455
1456
1457

Given the filtered source pool \mathcal{D} , we synthesize collage-style training images around one primary target (the image the model should attend to) and auxiliary fills (other images used to occupy remaining space and control background complexity). The full procedure is presented in Algorithm 1. Specifically, we sample and grid-quantize a canvas, then determine a feasible target scale by intersecting global bounds with a bbox-to-canvas cap and a minimum short-edge constraint after light aspect jitter (Steps 1–2). We plan & place the target using a fit-then-shrink heuristic with a single enlarge-canvas fallback (Steps 3–4). Remaining area is panelized into grid-aligned regions under simple aspect/size guards (Step 5). Panels are then filled (largest-first) by sampling images $\tilde{t} \in \mathcal{D}$ using usage-aware weights (favoring less-frequently used candidates) that also roughly match panel aspect; when needed, we apply a light center crop and bounded scaling (Step 6). If packing remains incomplete after a brief extra fill pass, we resample from the canvas; otherwise we finalize the collage (Steps 7–8). To avoid ambiguity when querying the target image, we annotate each collage tile with an ID and include this ID in the question as a reference. Figure 12 shows representative visualizations of synthesized collages.

1458 The canvas is sized so that the target box occupies only a tiny fraction of the canvas area, enforcing
 1459 $\text{area(bbox)}/\text{area(canvas)} < 0.0002$. We filter out items that vReasoner can already solve without
 1460 calling vSearcher using a pass@3 check (three attempts; any success leads to removal).
 1461

Algorithm 1 Target-and-Fill Collage Synthesis (High-level)

1462 **Require:** Metadata table \mathcal{D} (image path, W_{src} , H_{src} , object bbox), **target image** $t^* \in \mathcal{D}$, grid G , min
 1463 short edge M , canvas area/aspect ranges $[A_{\min}, A_{\max}]$ and $[a_{\min}, a_{\max}]$, target scale bounds
 1464 $[\lambda_{\min}, \lambda_{\max}]$, target aspect jitter τ_{tgt} , fill jitter τ_{fill} , fill scales $[\lambda_{\min}^{\text{fill}}, \lambda_{\max}^{\text{fill}}]$, panel aspect range
 1465 $[\text{AR}_{\min}^{\text{panel}}, \text{AR}_{\max}^{\text{panel}}]$, max effective source area S_{\max}^{eff} , **bbox coverage cap** $\rho_{\text{cap}}=2 \times 10^{-4}$, place-
 1466 ment retries R , max attempts T

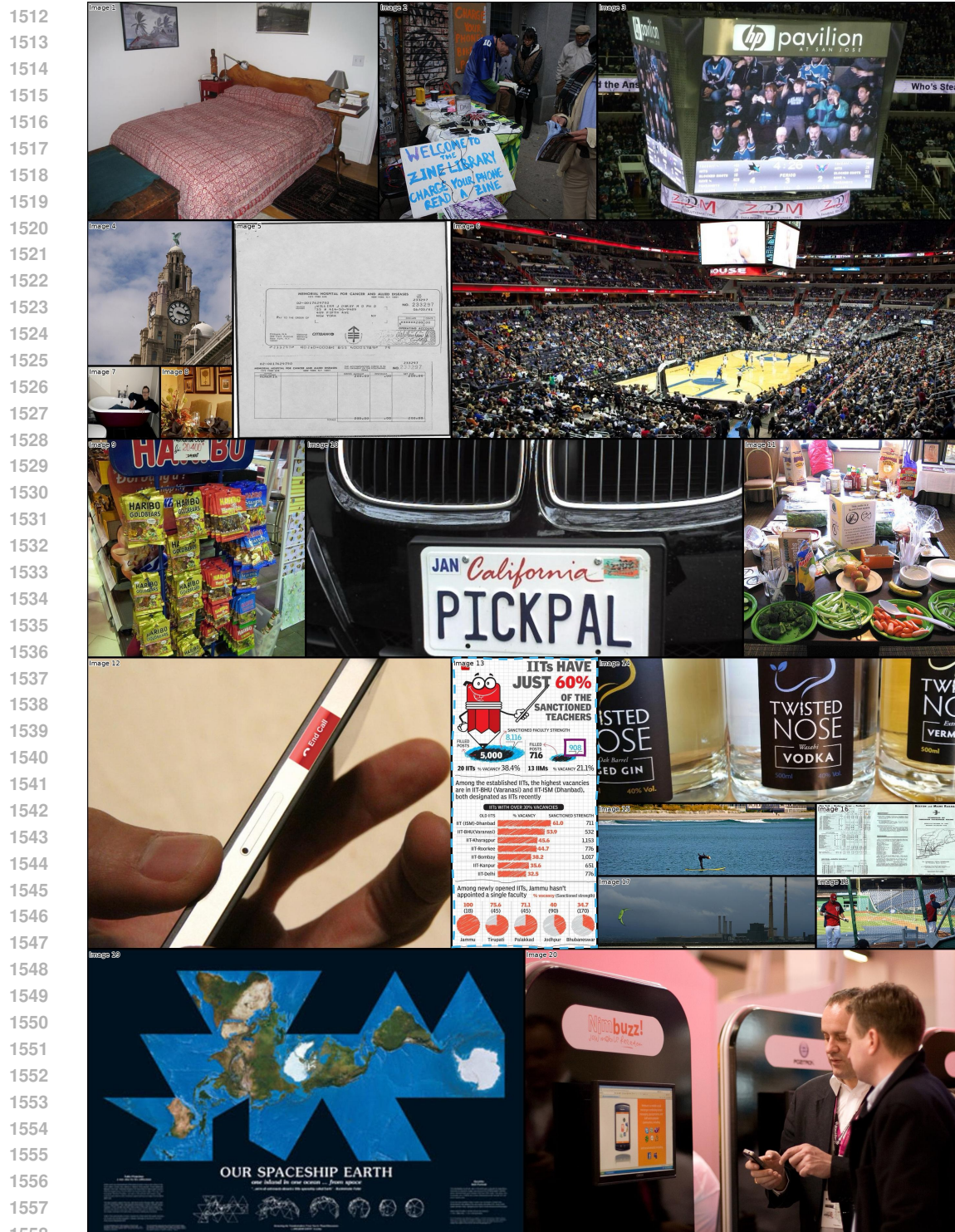
1467 **Ensure:** Canvas \mathcal{C} and placements $\mathcal{P} = \{\text{target, fills}\}$

- 1: **Precompute target meta.** From t^* , read W_{src} , H_{src} , bbox ratio ρ_{src} ; set $S_{\star} \leftarrow (W_{\text{src}} H_{\text{src}}) \cdot \min(1, \sqrt{S_{\max}^{\text{eff}} / (W_{\text{src}} H_{\text{src}})})^2$, and $r_{\text{src}} \leftarrow W_{\text{src}} / H_{\text{src}}$.
- 2: **for attempt** = 1 to T **do** ▷ rejection loop
- 3: **Step 1 — Sample canvas.** Draw $A_{\text{canvas}} \sim [A_{\min}, A_{\max}]$, $a \sim [a_{\min}, a_{\max}]$; snap to grid to obtain (W, H) .
- 4: **Step 2 — Compute feasible target scale interval.**
 Bounds: $\lambda \in [\lambda_{\min}, \lambda_{\max}]$; occupancy: $\lambda S_{\star} \leq A_{\text{canvas}}$; bbox: $\frac{\rho_{\text{src}} \lambda S_{\star}}{A_{\text{canvas}}} \leq \rho_{\text{cap}}$.
 Choose r_{\star} by log-jittering r_{src} within $\pm \tau_{\text{tgt}}$ and raise the lower bound on λ so that $\min(\sqrt{\lambda S_{\star}} r_{\star}, \sqrt{\lambda S_{\star}} / r_{\star}) \geq M$.
 Let I_{λ} be the intersection of the above constraints; if $I_{\lambda} = \emptyset$, optionally enlarge A_{canvas} once and recompute; if still empty, **continue** ▷ reject → restart at Step 1
- 5: **Step 3 — Plan target box.** Pick $\lambda \in I_{\lambda}$ (e.g., midpoint); set $w_{\star} = \sqrt{(\lambda S_{\star}) r_{\star}}$, $h_{\star} = \sqrt{(\lambda S_{\star}) / r_{\star}}$; snap (w_{\star}, h_{\star}) to multiples of G .
- 6: **Step 4 — Place target.** Best-fit on the free list (grid-aligned). If no fit, iteratively shrink (w_{\star}, h_{\star}) and update $\lambda = w_{\star} h_{\star} / S_{\star}$, keeping feasibility in I_{λ} , up to R retries; if still not placed, optionally enlarge canvas once and re-plan; if it fails, **continue** ▷ reject → restart at Step 1
- 7: **Step 5 — Normalize free space.** Recursively split free regions into grid-aligned panels subject to aspect $\text{AR}_P \in [\text{AR}_{\min}^{\text{panel}}, \text{AR}_{\max}^{\text{panel}}]$ and minimal size.
- 8: **Step 6 — Fill panels.** For each panel (largest-first), sample a fill image $\tilde{t} \in \mathcal{D}$ within a $\pm \tau_{\text{fill}}$ aspect band around AR_P ; if needed, center-crop \tilde{t} to AR_P ; scale with $\lambda_{\text{fill}} \in [\lambda_{\min}^{\text{fill}}, \lambda_{\max}^{\text{fill}}]$ and place.
- 9: **Step 7 — Resample if needed.** If residual free space remains after one extra fill pass, **continue** ▷ reject → restart at Step 1
- 10: **Step 8 — Finalize. return** \mathcal{C}, \mathcal{P}
- 11: **end for**
- 12: **return** **None** ▷ no feasible collage after T attempts

1499
 1500
C.2 OUT-OF-LOOP RL DATA

1501 For PP-DocLayout_plus-L, we use the following configuration: `{"threshold": 0.01, "layout_nms": True, "layout_merge_bboxes_mode": "union"}`.

1502 To construct meaningful visual search targets from the boxes produced by PP-DocLayout_plus-L, we start by dropping boxes of trivial layout classes such as header and footer, keeping only text, image, table, chart, figure_title, and paragraph_title boxes. We then drop boxes that are too large as they usually merge disparate things together. Boxes with area larger than a quarter of the whole image area are dropped, except for charts which are usually clean and we use a much higher threshold (0.8) for them. Next, we merge boxes that are very close to each other, measured by the effort required to enclose them in one box. The effort is computed as $1 - \text{summed_area} / \text{min_enclosing_area}$. We start with the boxes that require the



Question: In image13, what is the sanctioned faculty strength in 13 IIMS?

Answer: 908

Target Image Target Bbox

Figure 12: Example of synthesized collage for the in-loop RL. Multiple low-resolution images are stitched to raise visual density. The blue dashed box highlights the target tile; the magenta box marks the target bbox. Remaining tiles are distractors.

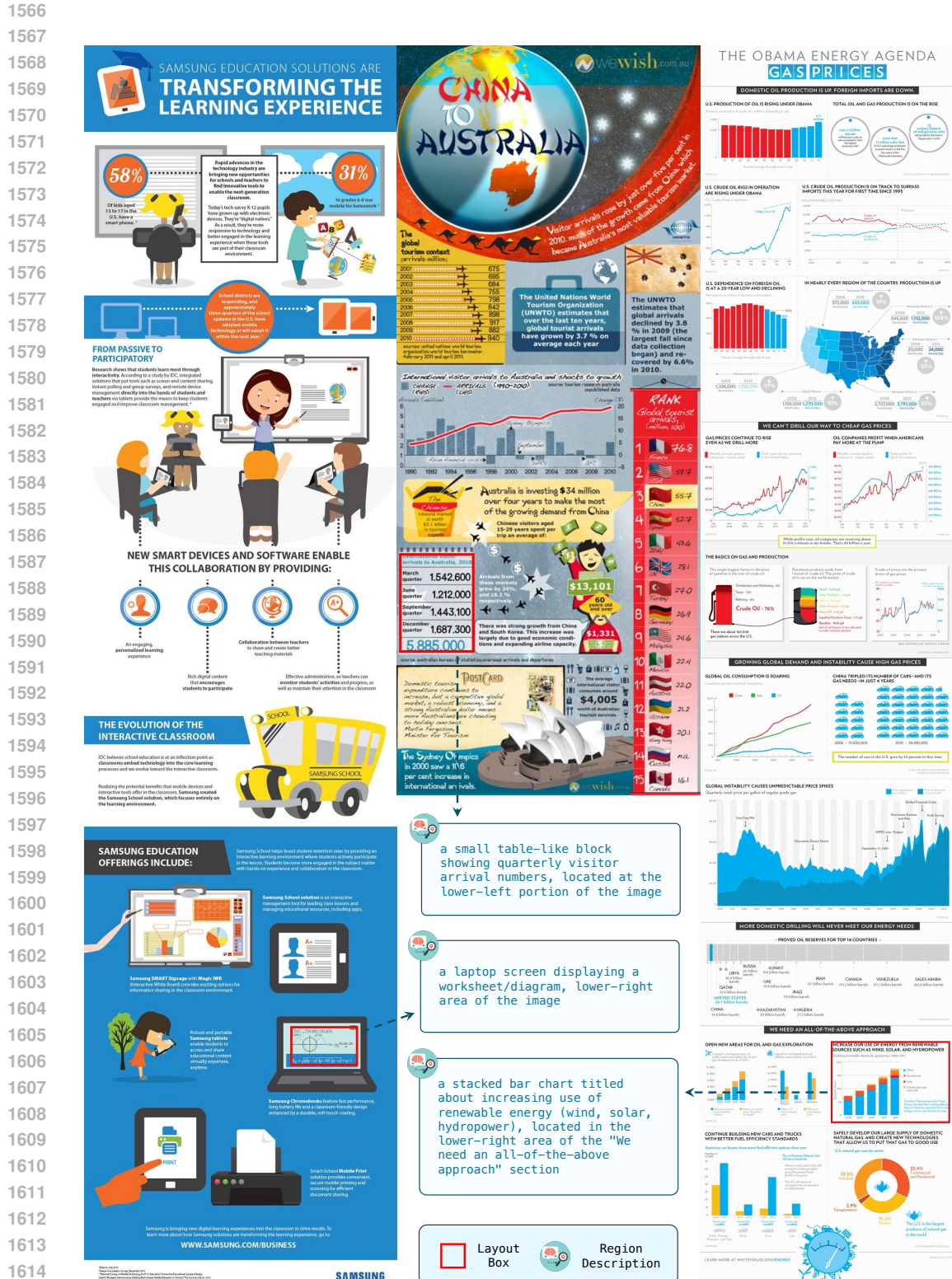


Figure 13: Examples of InfographicVQA images with pre-generated layout boxes and region descriptions for the out-of-loop RL.

1620 least effort to merge, and stop until the required effort reaches a threshold. For `figure_title`
 1621 and `paragraph_title` boxes, the threshold is 0.15, while for other boxes, it is 0.1. This helps
 1622 merging small, auxiliary boxes such as figure titles and chart legends with their closest neighbors in
 1623 the vicinity, avoiding truncating important context and preventing trivial search targets dominating
 1624 the dataset. We skip a merge if the new box would be too large (box-to-image area ratio more than
 1625 0.25) or have an extreme aspect ratio (not within 1:5 and 5:1). We do not merge charts and tables.

1626 After merging the boxes, we drop (1) charts/tables enclosing other charts/tables, (2) unmerged im-
 1627 ages that do not contain any text or titles, (3) unmerged titles, (4) unmerged texts, (5) boxes that are
 1628 too small (box-to-image area ratio less than 0.001), and (6) boxes with extreme aspect ratios (not
 1629 within 1:5 and 5:1). These boxes often contain little information (e.g., icons, short texts). In the end,
 1630 an image may still have multiple visual search targets; they are treated as separate data entries.

1631 To generate region descriptions for the visual search targets obtained earlier, we first draw a red box
 1632 around the target on the image, and then prompt GPT-5-nano as follows:
 1633

1634 [SYSTEM]
 1635 You are a visual assistant. Your goal is to help the user to locate the region indicated by
 1636 the red bounding box in an image.
 1637 When the user asks you to describe the region, you must follow the following rules:
 1638 - Keep it super simple and short as if you can't see clearly what is in the region.
 1639 - Don't mention any details, specific content, or small text in the region.
 1640 - Use concise, visually grounded targets (e.g., a chart, an object, a text block, a
 1641 distinct area).
 1642 - Optionally include approximate location (e.g., top-left of the image, bottom-right of the
 1643 big chart, center column).
 1644 - Optionally include the title of the region (e.g., the table about XXX, the section titled
 1645 XXX).
 1646 - Avoid non-visual or ordinal references (e.g., "the third largest bar", "the second row's
 1647 number").
 1648 - Don't mention the red bounding box.
 1649 Output format: `region_description={...}`
 1650 [USER]
 1651 Describe the region in the red bounding box.
 1652

1650 In Figure 13, three examples of the final data are shown. Note that unlike collages, these examples
 1651 are not stitched together; they are simply displayed side-by-side to save space.
 1652

1653 D INSIGHT-O3 IMPLEMENTATION DETAILS

1654 The maximum image resolution of vSearcher is set to ~ 3.2 M pixels (4K tokens/image) during training,
 1655 and ~ 12.8 M pixels (16K tokens/image) during evaluation. Oversize images are downsampled
 1656 to meet the constraint. We allow both vReasoner and vSearcher to make at most 6 sub-agent/tool
 1657 calls during both training and evaluation. Image crops returned by sub-agent/tool calls are obtained
 1658 from original images, and then resized if they exceed the size limit. For vSearcher, we use a max-
 1659 imum response length (including results returned by sub-agent/tool calls) of 9K and 32K tokens
 1660 for training and evaluation, respectively. The sampling temperature of vSearcher is set to 1 and 0,
 1661 respectively. Other hyperparameters include: training batch size 24, rollout number 8, learning rate
 1662 10^{-6} , KL loss coefficient 0.01, reward weights $\lambda_{\text{format}} = 0.2$, $\lambda_{\text{IoU}} = 0.8$, and IoU reward threshold
 1663 $\alpha = 0.25$. The composition of in-loop/out-of-loop training data is 1:1. We train vSearcher fully on-
 1664 policy for 150 steps. We freeze the vision tower and the adapter of Qwen2.5-VL-7B-Instruct during
 1665 the whole training process. We use GPT-5-nano (OpenAI, 2025a) for evaluating answer correctness.
 1666 Our code is based on verl (Sheng et al., 2024). The prompts we use can be found in Appendix I.
 1667

1668 E MORE VISUALIZATIONS OF INSIGHT-O3 REASONING PROCESS

1669 Figure 14 and 15 show examples of inference process of INSIGHT-O3 (GPT-5-mini as vReasoner).
 1670 The vReasoner issues natural-language target descriptions; the vSearcher localizes evidence and
 1671 returns them. Across a few rounds, the pair composes multi-step evidence and produces the final
 1672 answer, demonstrating that INSIGHT-O3-VS plugs in cleanly and supports effective reasoning.
 1673

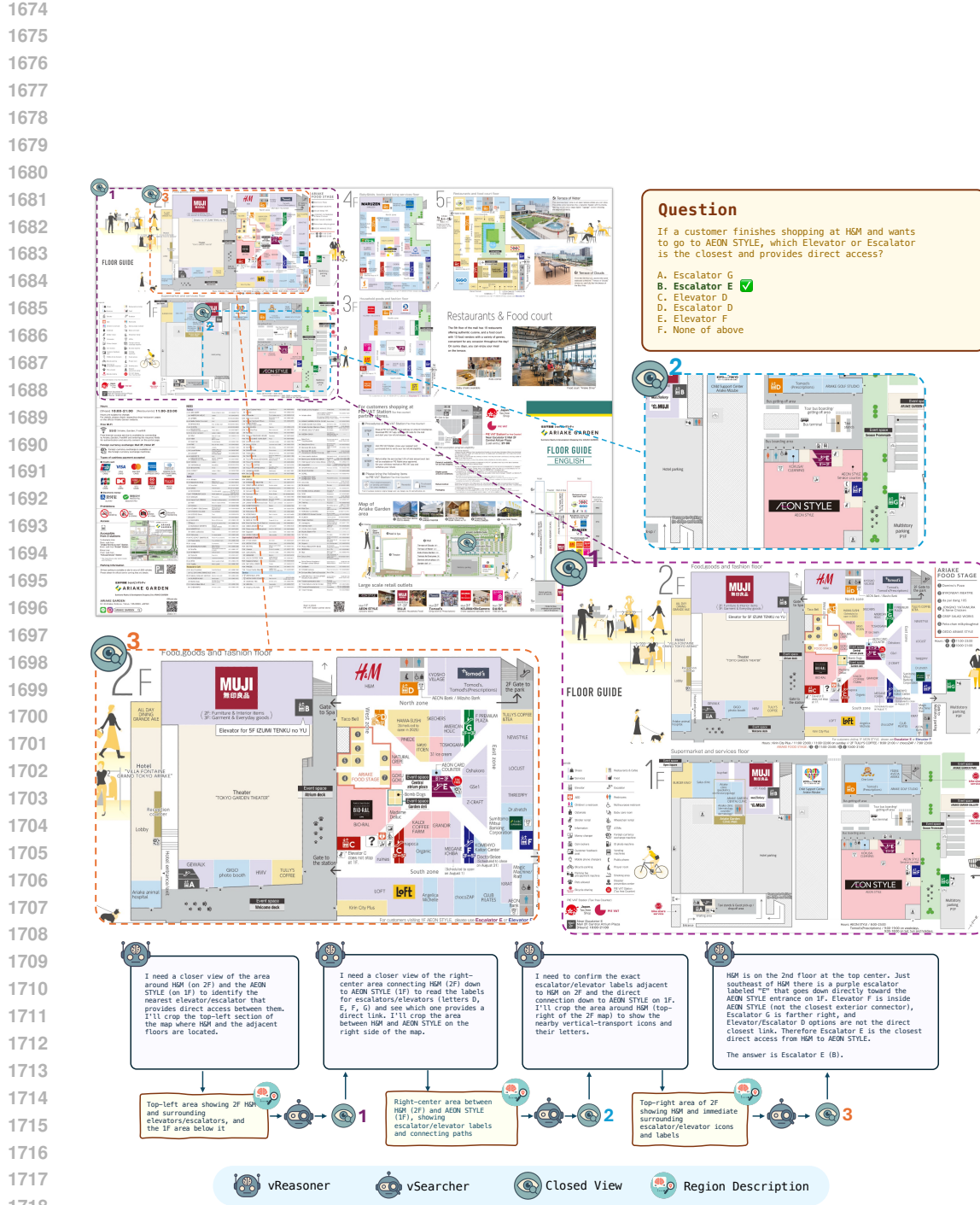


Figure 14: Qualitative result 1 with GPT-5-mini as vReasoner and INSIGHT-O3-vS as vSearcher. The reasoner requests venue-level cues (e.g., legend/index lookups); the searcher returns localized regions and snippets, iterating to a correct answer.

1728
1729
1730
1731
1732
1733

1734
1735
1736
1737
1738
1739
1740
1741
1742
1743
1744
1745
1746
1747
1748
1749
1750
1751
1752
1753
1754
1755
1756
1757
1758
1759
1760
1761
1762
1763
1764
1765
1766
1767
1768
1769
1770
1771
1772
1773
1774

1775
1776
1777
1778
1779
1780
1781



Figure 15: Qualitative result 2 with GPT-5-mini as vReasoner and INSIGHT-O3-vS as vSearcher. The reasoner requests venue-level cues (*e.g.*, legend/index lookups); the searcher returns localized regions and snippets, iterating to a correct answer.

1782 F COMPARATIVE ANALYSIS BETWEEN INSIGHT-O3 AND BASELINES

1784 In Figure 16-19, we compare the behavior of INSIGHT-O3 (GPT-5-mini + InSight-o3-vS) with two
 1785 baselines: (1) GPT-5-mini and (2) GPT-5-mini + Qwen2.5-VL-7B. This comparative analysis is
 1786 based on three examples of O3-BENCH. We rate each crop returned by vSearcher on three levels:
 1787

- 1788 • High-quality crops tightly enclose the visual search targets and the relevant context.
- 1789 • Medium-quality crops contain the visual search targets but include too much context.
- 1790 • Low-quality crops miss or truncate the visual search targets or relevant context.
- 1791

1792 In the most basic setting where vReasoner does not have access to vSearcher, it often uses similar
 1793 reasoning patterns as follows to reach its conclusion: “I first locate … I see … I then look for
 1794 … There is … Therefore …” (see the top parts of Figure 17-19). During this process, vReasoner
 1795 often hallucinates and makes factual errors about what it sees, suggesting that it does not really see
 1796 the relevant visual details clearly but still pretends so anyway.

1797 With the vanilla Qwen2.5-VL-7B vSearcher, vReasoner is able to take closer looks at regions of
 1798 interest and makes less factual errors (see the bottom part of Figure 17 and the middle part of
 1799 Figure 18-19). However, the vanilla vSearcher is often unreliable, returning inaccurate/wrong crops
 1800 to vReasoner or simply concluding that the target is not in the image, usually after a minimal amount
 1801 of (sometimes none) reasoning. In such cases, vReasoner would eventually give up and resort to its
 1802 own perception after multiple failed visual search attempts, leading to wrong final answers.

1803 In comparison, our visual search agent, InSight-o3-vS, would usually first reason about the visual
 1804 search request and then crop the candidate region to verify before returning it to vReasoner. For
 1805 example, in Figure 16, InSight-o3-vS first reasons about what the bounding box should cover:

1806 Based on the description, the right section of the map includes the
 1807 legend/index and the “Catering venues” list with numbered cafes. The
 1808 legend/index is located at right of the map, and the “Catering venues”
 1809 list is further down, under the “Catering venues” heading. The bounding
 1810 box should cover these areas.

1811 Then, after viewing the cropped region, it concludes:

1813 Based on the tool response, the right section of the map showing the
 1814 legend/index and the “Catering venues” list with numbered cafes is
 1815 already covered by the bounding box provided. Therefore, no further
 1816 zooming is necessary.

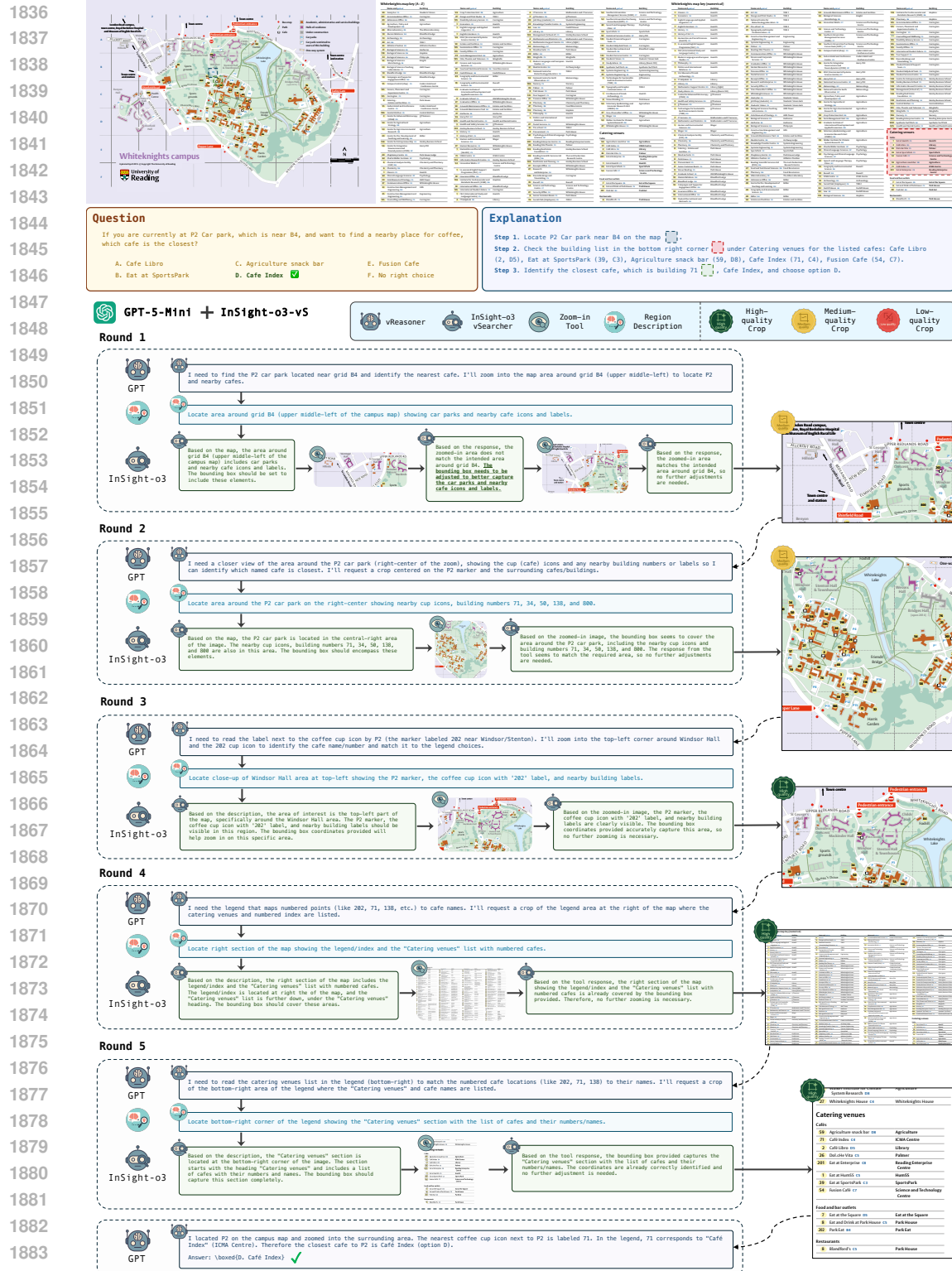
1817 In some cases, InSight-o3-vS is able to correct an initial bad crop after reviewing the crop:

1818 Based on the response, the zoomed-in area does not match the intended
 1819 area around grid B4. The bounding box needs to be adjusted to better
 1820 capture the car parks and nearby cafe icons and labels.

1822 The returned crops are usually medium-to-high-quality crops as shown in Figure 16. From these
 1823 cases, we can see that vSearcher mostly helps vReasoner by (i) precisely locating the regions re-
 1824 quested by vReasoner and (ii) presenting them to vReasoner and directing its attention to those
 1825 regions, thereby reducing hallucination and facilitating evidence-based reasoning.

1827 G FAILURE CASES OF INSIGHT-O3

1829 Figure 20-21 show typical failure cases of INSIGHT-O3. In the first three failure cases, vSearcher
 1830 (InSight-o3-vS) provided the correct crops for the search targets but vReasoner (GPT-5-mini) an-
 1831 swers incorrectly due to its own errors, e.g., ignoring visual evidence due to internal knowledge bias,
 1832 and jumping to conclusion without examining key visual information. This suggests that existing
 1833 frontier models, even the proprietary ones, are still not very good at thinking with images in com-
 1834 plex scenarios. The last failure cases is due to vSearcher failing to understand the structure of the
 1835 map and/or the relatively complicated region descriptions involving multiple visual cues. Finally,
 we note that, at least on O3-BENCH, most wrong answers are due to vReasoner, not vSearcher.



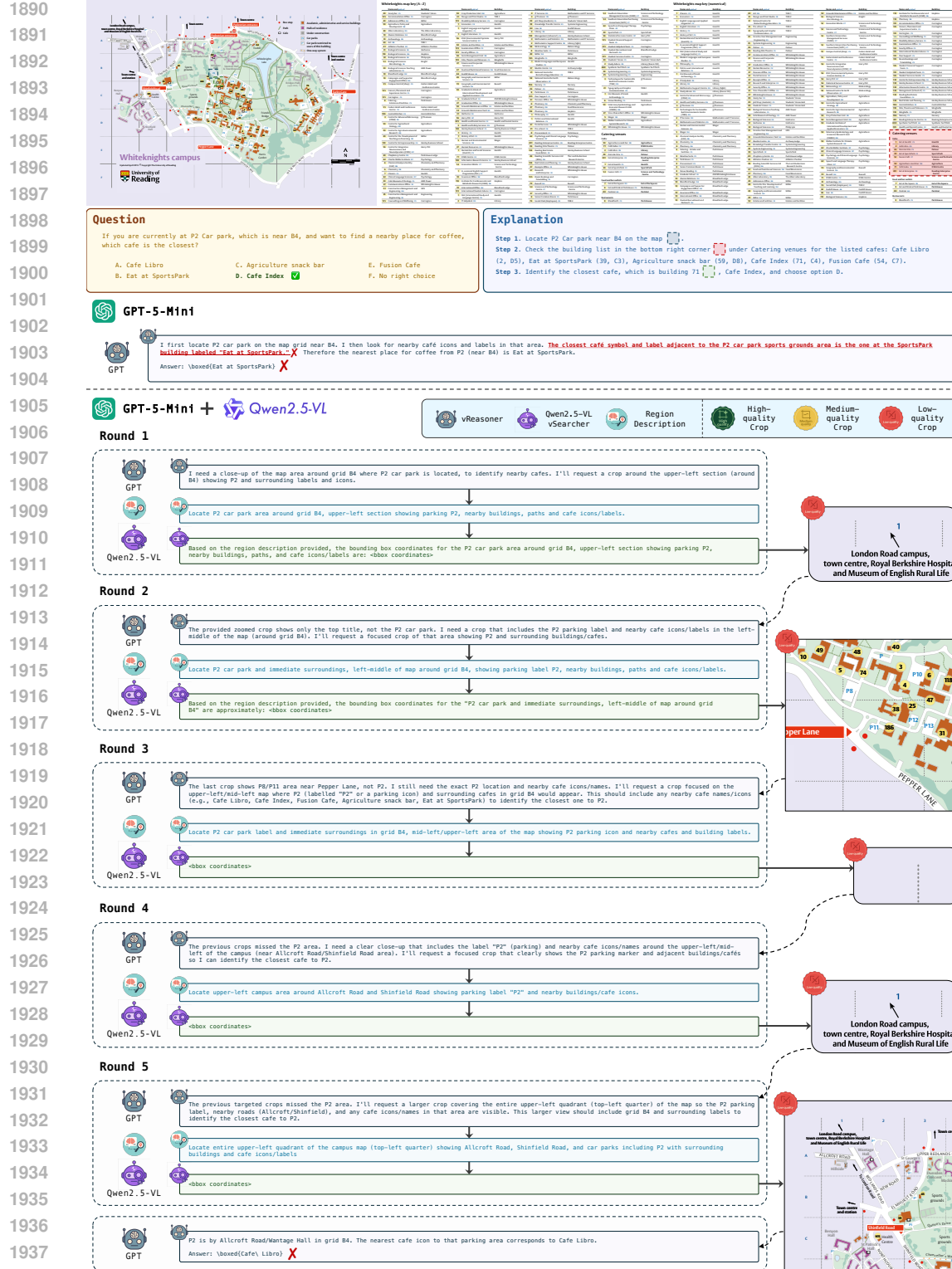


Figure 17: Example 1 (MAP case 1, continuation of Fig. 16): reasoning traces of GPT-5-mini and GPT-5-mini + Qwen2.5-VL-7B-Instruct. GPT-5-mini exhibits misperception and reasoning drift, while Qwen2.5-VL-7B-Instruct frequently fails to follow vReasoner’s instructions, producing low-quality crops misaligned with the described regions. Consequently, both baselines yield incorrect answers.

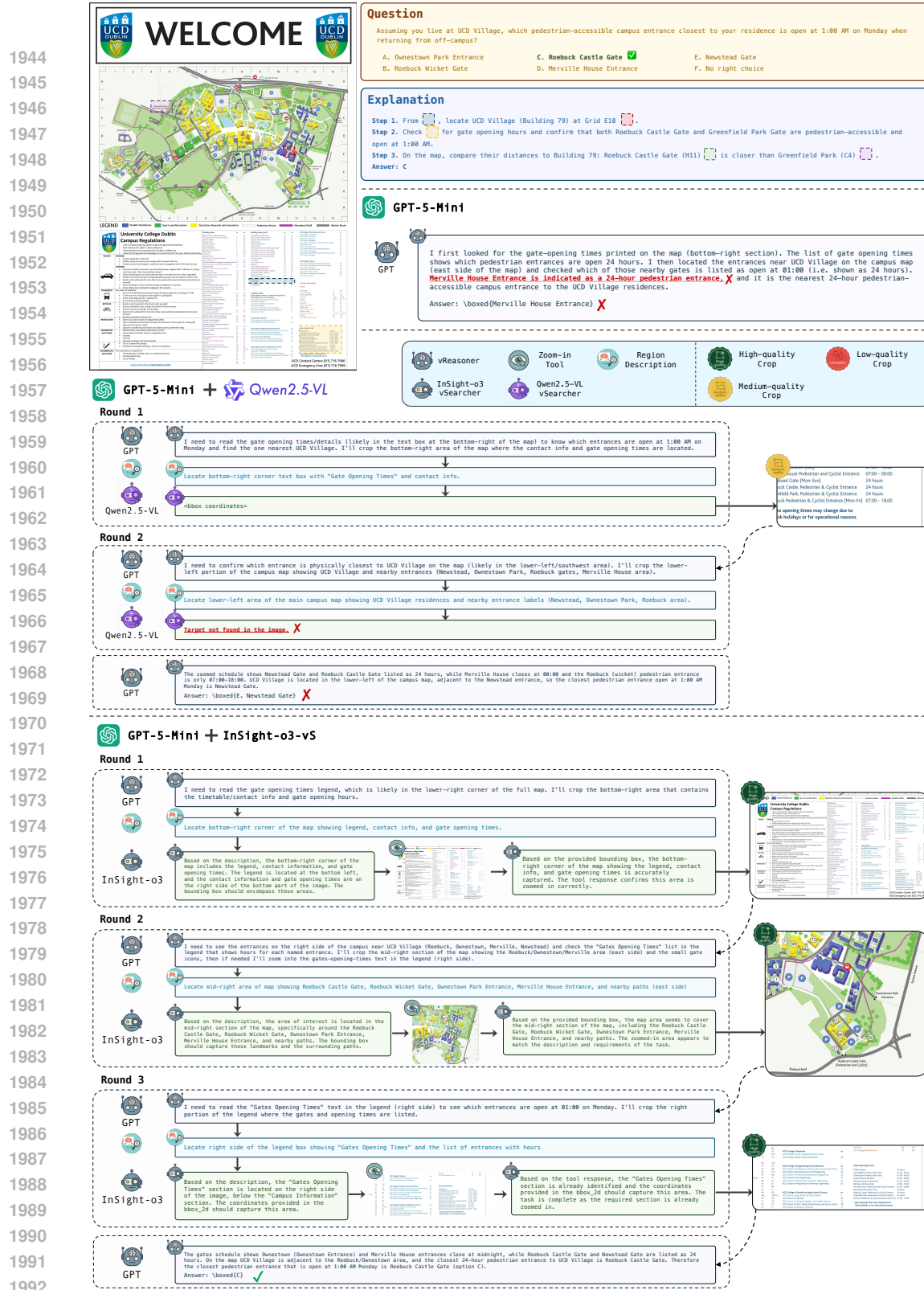


Figure 18: Example 2 (MAP case 2): reasoning traces of our model, GPT-5-mini, and GPT-5-mini + Qwen2.5-VL-7B-Instruct. Our INSIGHT-O3-VS accurately follows vReasoner’s instructions and returns high-quality crops aligned with the described regions, leading to a correct answer. In contrast, Qwen2.5-VL-7B fails to return a valid crop in the final reasoning round, resulting in an incorrect answer.

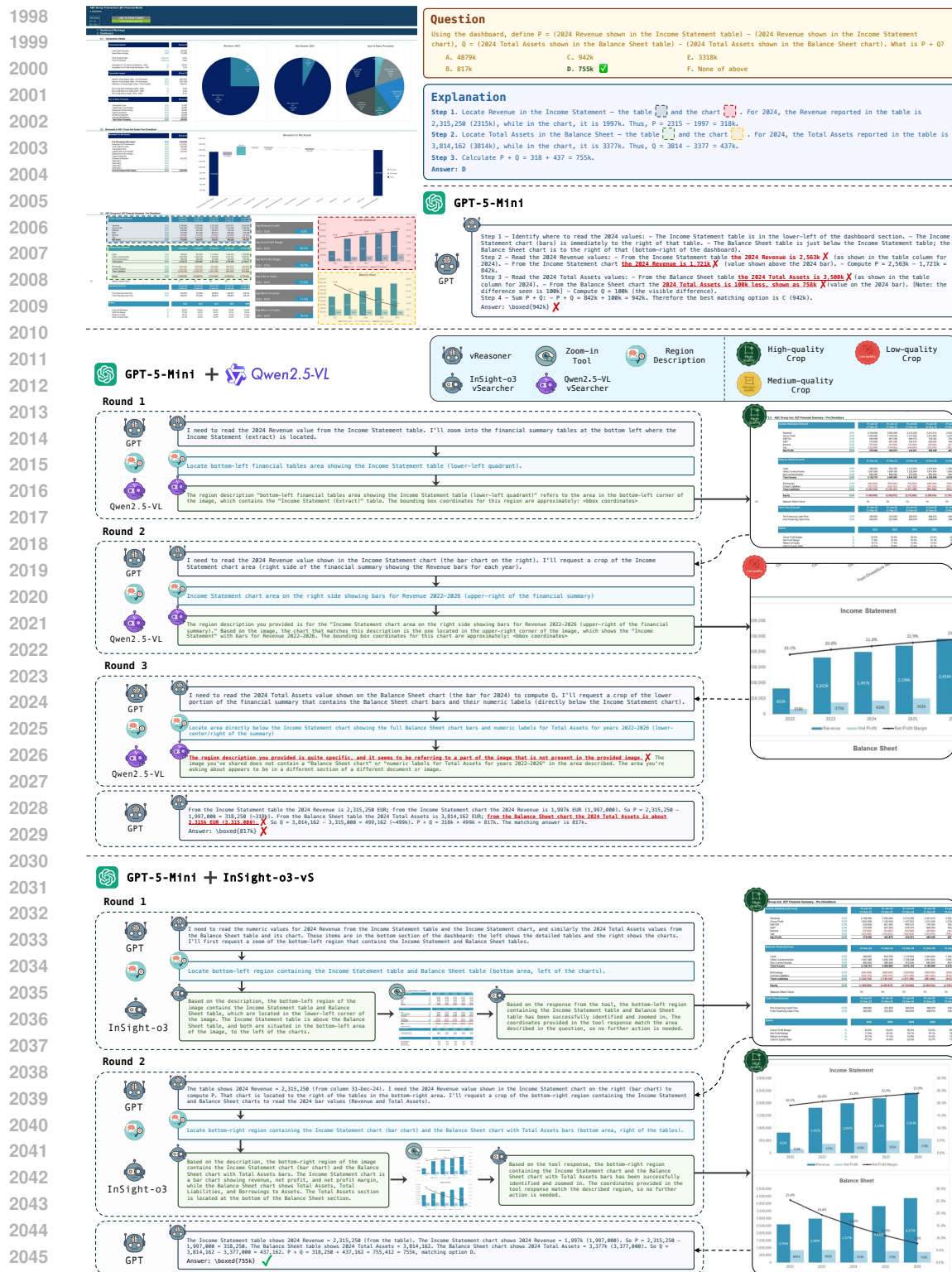


Figure 19: Example 3 (CHART case): reasoning traces of our model, GPT-5-mini, and GPT-5-mini + Qwen2.5-VL-7B-Instruct. INSIGHT-O3-VS effectively follows vReasoner’s guidance and retrieves high-quality crops that fully capture the described regions. In contrast, Qwen2.5-VL-7B returns only partial crops in Round 2 and, in the Round 3, fails to produce a valid crop as requested by vReasoner, incorrectly concluding that the target region is absent, which leads to an incorrect answer.

2106

2107

2108

Failure case 3 (vReasoner – Improper Search Delegation)



Question

A person starting from the Electric Vehicle Parking/Charging Stations wants to reach the Corewell Health Kids' Port. Which of the following locations/facilities would they pass directly along the most direct route to the Kids' Port?

A. Market Place C. GRR Life Market & Cafe E. Taxi Stand
 B. Baggage Claim No.4 D. ATM F. No right choice

Explanation

Step 1. From the legend, identify the symbols for Electric Vehicle Parking/Charging Stations and Corewell Health Kids' Port.

Step 2. On the terminal map, locate the Electric Vehicle Parking/Charging Stations  in the bottom-left corner, and the Corewell Health Kids' Port  in the center of the terminal.

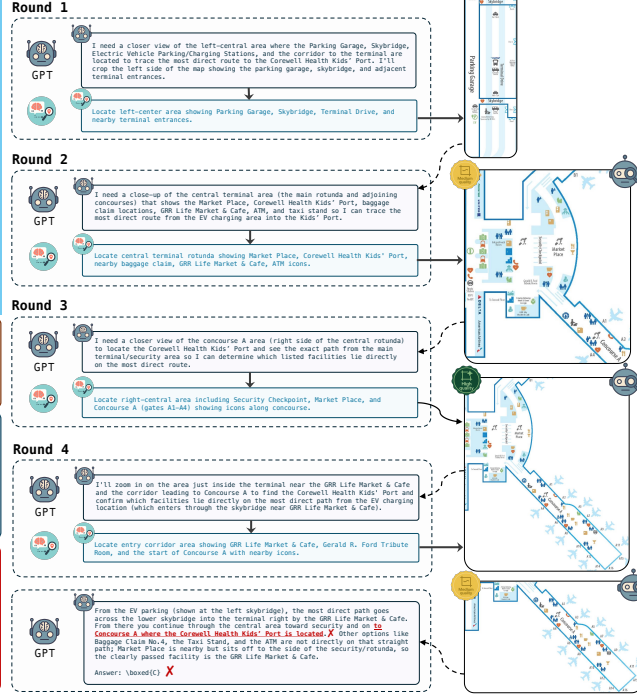
Step 3. Starting from the Electric Vehicle Parking/Charging Stations, cross the Skybridge into the terminal, pass by the ATM near the entrance, then continue forward and turn left to reach the Corewell Health Kids' Port.

Answer: D (ATM)

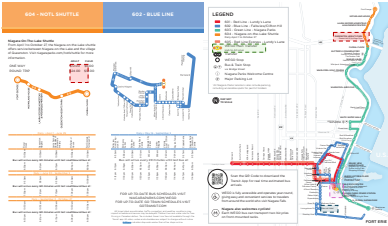
Failure Reason

This failure stems from the vReasoner's inability to localize the target region Corewell Health Kids' Port. Instead of first consulting the legend to identify the target's symbol, the vReasoner attempts direct visual search across multiple regions without delegating the task to the vSearcher. During this process (Round 1), it generates several broad region descriptions. Although the vSearcher returns crops that match these descriptions, the target occupies only a small portion of each large region and lacks textual labels, making recognition difficult. Consequently, even with the cropped images, the vReasoner fails to identify the target and produces an incorrect answer.

A more effective strategy would be for the vReasoner to reference the legend first and delegate precise localization to the vSearcher.



Failure case 4 (vSearcher – Region Localization Failure)



Question

If I am staying at the Marriott Hotel and plan to go to QUEENSTON HEIGHTS PARK today, can I reach it directly by transferring between buses (without walking in between)? And how many lines must I take at minimum?

A. No, 2 lines C. Yes, 1 line E. Yes, 3 lines G. None of the above
 B. No, 3 lines D. Yes, 2 lines F. None of the above

Explanation

Step 1. Locate the Marriott Hotel  near the area below the blue line.

Step 2. Locate QUEENSTON HEIGHTS PARK  at the top of the map near the orange line.

Step 3. Determine the route: take the blue line, transfer to the green line, and then transfer to the orange line.

Step 4. Refer to the LEGEND and note that the Main Transfer  allows transfers to all lines. Transfer from the blue line to the green line at Main Transfer , and then from the green line to the orange line at FLORAL CLOCK.

Step 5. Conclude that it is possible to reach the destination directly via transfers, requiring three lines.

Answer: E.

Failure Reason

In this case, the vReasoner correctly decomposes the question and provides a clear region description that specifies both the target area and its approximate location. However, due to the complex visual structure of the image, the vSearcher fails to retrieve the correct region as instructed. Despite multiple clarifications and follow-up attempts from the vReasoner, the vSearcher still cannot locate the intended area. As a result, the vReasoner ultimately relies on its own limited visual perception to answer, leading to an incorrect localization of Queenston Heights Park.

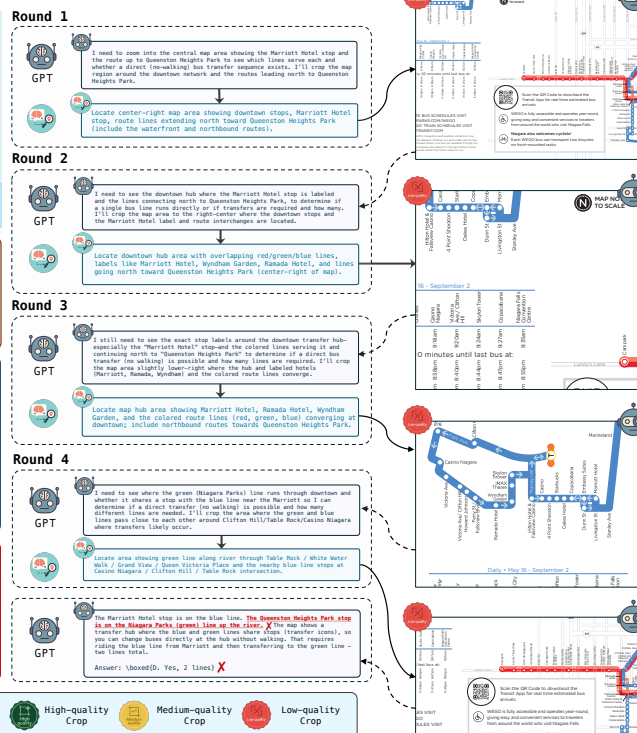


Figure 21: Failure cases 3 & 4 of INSiGHT-o3 (GPT-5-mini + InSight-o3-vS).

2160 H PROMPTS FOR O3-BENCH

2162 H.1 PROMPTS FOR INFORMATION EXTRACTION

2164 For both the full image and cropped images, we feed them into Qwen2.5-VL-32B (Bai et al., 2025)
 2165 for information extraction using the same prompt as below.

```

2166     ### System
2167
2168     You are acting as a **precise visual information extractor**.
2169     Given ONE image, you must (1) identify the image type, (2) write a **comprehensive,
2170     strictly factual** caption, and (3) extract **complete OCR text** when present (with
2171     special handling for tables).
2172     Follow the rules **exactly** and return the output in the three sections shown under **Output Format**.
2173
2174     ---
2175
2176     ### Global Principles
2177
2178     1) **No hallucinations.** Describe only what is visible. If something is unclear, write '[  

2179     illegible]' or '[partially obscured: ...]'.
2180     2) **Be exhaustive.** Do not omit small text, legends, tick labels, footnotes, watermarks,
2181     axis titles, subtitles, panel labels (e.g., '(a)', '(b)'), or figure notes.
2182     3) **Preserve fidelity.** Copy punctuation, capitalization, diacritics, signs ('+', '-'),
2183     units, and spacing **exactly**. Do not normalize numbers or rewrite text.
2184     4) **Reading order.** When listing text outside of tables, use **top-to-bottom, left-to-
2185     right** order.
2186     5) **Language.** OCR text must remain in the **original language(s)**. The caption should
2187     be in English unless the visible UI/page language is clearly not English; in that case,
2188     keep captions in that language. Do **not** translate OCR unless the image itself contains a
2189     translation.
2190     6) **No extra sections.** Output **only** the three required sections and nothing else.
2191
2192     ---
2193
2194     ### Image Type Identification (Section 1)
2195
2196     - Classify the image using one or more of the following types (multiple allowed if
2197     appropriate):
2198         'chart', 'table', 'document/text page', 'diagram/flowchart', 'map', 'UI/screenshot', ' '
2199         'form', 'invoice/receipt', 'poster/flyer', 'scientific figure (multi-panel)', 'natural
2200         scene', 'legend', 'infographic', 'other (specify)'.
2201
2202     ---
2203
2204     ### Detailed Caption (Section 2)
2205
2206     Write a **dense, structured** caption that covers all critical elements. Use clear,
2207     objective language and organize logically (left->right, top->bottom; or foreground->
2208     background). Include the relevant sub-guidelines:
2209
2210     **A. Charts / Plots / Scientific Figures**
2211     - State the figure title (if present), chart type(s), axes titles, **units**, tick labels,
2212     gridlines, data series, markers/line styles, **legend and color/shape mappings**,
2213     annotations, error bars, trend lines, and notable extrema/patterns (peaks, troughs,
2214     monotonic trends, outliers).
2215     - If multi-panel: identify panel labels '(a)', '(b)', ... and summarize each panel in order
2216     .
2217     - Mention any insets, callouts, footnotes, or sources.
2218
2219     **B. Tables / Forms / Receipts / Documents**
2220     - Summarize what the table/document contains (topics/fields), approximate dimensions (e.g.,
2221         '12 rows x 6 columns'), header rows, merged cells, checkboxes, stamps, signatures, page
2222         numbers, and footers/footnotes.
2223     - Call out key sections (headings, lists, paragraphs), logos, and seals.
2224
2225     **C. Maps**
2226     - Report title, compass/north arrow, scale/scale bar, coordinate grid or lat/long,
2227     boundaries, regions, routes/lines with **color-to-meaning mapping** (from legend), symbols/
2228     icons (e.g., hospitals, stations), labels for places/roads, insets, and any zoning/heat
2229     color ramp.
2230     - Include legend content (categories and their visual encodings).
2231
2232     **D. UI / Screenshots**
  
```

```

2214 - App/site name, window title, menus/toolbars, visible controls (buttons, toggles,
2215 checkboxes, dropdowns, search fields), selected/disabled states, scroll position,
2216 timestamps, status bars, notifications, dialogs, visible file paths, and version strings.
2217
2218 **E. Natural / Real-World Scenes**
2219 - Enumerate salient objects, text on signs/labels, relative positions (e.g., 'a red sign
2220 above the doorway'), counts for repeated items, conditions (day/night, indoor/outdoor), and
2221 visible brands/logos.
2222 > Do **not** invent interpretations or causal explanations. Keep to what is visually
2223 supported.
2224
2225 ---
```

OCR Extraction (Section 3)

Extract ****all visible text****. Follow these rules:

****General OCR Rules****

- Use ****natural reading order**** (top->bottom, left->right).
- Preserve original line breaks and spacing.
- If text is repeated (e.g., in a watermark), list it once and note '(repeats)' if necessary.
- If a character/word is uncertain, write it as '[illegible]' or '[?]' without guessing.

****Tables (very important)****

- When an area is a table, extract it immediately using ****Markdown table syntax****.
- Preserve the ****exact**** row/column structure and header rows; if a cell has line breaks, use '
' or '\n'.
- For merged cells, repeat the visible text in each affected cell and note '(merged)' once after the table.
- If multiple tables exist, label them sequentially as 'Table 1', 'Table 2', ... in the order they appear.

****Documents / Text Pages / Forms****

- Extract headings, paragraphs, lists, captions, footnotes, headers/footers exactly as shown. Maintain indentation and list markers.

****Charts / Maps / Diagrams / UI / Natural Scenes****

- Extract ****all textual elements**** present: titles, subtitles, axis labels, tick labels, legend entries, series labels, annotations, callouts, map labels (places/roads/lines), UI labels (menu items, buttons, tooltips), signs, badges, and watermarks.

If ****no text**** is present, write 'None'.

Output Format (return EXACTLY this Markdown structure; no code fences)

Image Identification
<one or more types from the allowed list; add brief justification if mixed>

Detailed Caption
<dense, strictly factual caption covering all visible elements per rules above>

Extracted OCR (if any)
<EITHER: full Markdown tables + remaining text in reading order; OR: all non-table text in reading order; write "None" if no text>

H.2 PROMPTS FOR CONSTRUCTING O3-BENCH

For chart images, we use the following prompt for GPT-5 (OpenAI, 2025a) to automatically generate QA instances.

You are an expert assessment-item author who designs rigorous ****multi-hop visual-reasoning**** questions to benchmark "think-with-images" abilities on ****dense diagrams, charts, tables, and schematics****. The goal is to generate items so challenging that today's strongest MLLMs score ****<= 50%**** without external tools.

You will receive:

INPUTS

1. ****GLOBAL_OCR**** - OCR or caption text describing the entire image/page.
{GLOBAL_OCR}
2. ****GLOBAL_CAPTION**** - caption text describing the entire image/page.
{GLOBAL_CAPTION}

```

2268
2269 3. **LAYOUTS** - a list of cropped regions. Each layout contains:
2270   - 'layout_id' - unique numeric ID (for your internal reference only).
2271   - 'caption_or_ocr' - OCR or descriptive caption of the cropped region.
2272   {LAYOUTS}
2273
2274 > **Important constraint:**  

2275 > In the **question** and **options**, you must use only natural labels/text present in the  

2276   'GLOBAL_OCR' or 'GLOBAL_CAPTION' or 'caption_or_ocr'.
2277 > **Never** mention 'layout_id', 'region', 'crop', 'panel', 'box', or any similar tokens.  

2278 Layouts are **reference-only** to help you construct questions; they may be cited in the **  

2279 explanation** but not in the question or options.
2280
2281 ---
2282
2283 ## TASK
2284 Create **3-5 independent multiple-choice questions** that each requires **>=2 distinct  

2285 visual hops** across layouts or global text. These must be **multi-step items directly**,  

2286 not derived from single-step seeds. All facts must be grounded in the provided OCR/captions  

2287 only.
2288
2289 ---
2290 ## QUESTION-DESIGN RULES
2291 1. **Multi-hop inference (required)**
2292   Each question must integrate information from at least **two different layouts** or from  

2293   global + local text. Valid patterns include:
2294   - Cross-table lookup & join (match category in Layout A to code/key in Layout B, then  

2295     filter by condition).
2296   - Table <-> chart alignment (map series/labels from one layout to another).
2297   - Diagram <-> table mapping (use schematic labels to query corresponding rows/values).
2298   - Temporal alignment (identify when a threshold is crossed in one chart, then fetch  

2299     related info from another).
2300   - Proportions/ratios/ranks (compute shares from one region and compare with targets in  

2301     another).
2302   - Exceptions/constraints (apply footnote conditions from one layout before interpreting  

2303     values elsewhere).
2304
2305 2. **Analytical realism**
2306   Situate each question in a plausible scenario (finance, science, education, operations,  

2307   product metrics, etc.) while remaining strictly grounded in the provided OCR/captions.
2308
2309 3. **Difficulty control**
2310   Questions should require careful scanning, cross-referencing, and light calculations (brackets,  

2311   differences, ratios, ranking). Avoid items that can be answered at a glance.
2312
2313 4. **Units, scales, rounding**
2314   Always follow the units/scales given in the OCR. If rounding is necessary, state the  

2315   rounding rule in the **explanation**.
2316
2317 5. **Ambiguity guardrails**
2318   Ensure exactly **one correct choice** among A-E, unless 'F' ("No right choice") is  

2319   correct. Adjust conditions to avoid ties.
2320
2321 6. **Label fidelity**
2322   Copy text exactly as provided (case, spelling, diacritics). Never use external/world  

2323   knowledge.
2324
2325 ---
2326
2327 ## ANSWER-OPTION RULES
2328 1. Provide **exactly six** options, one per line, labeled 'A.' ... 'F.'
2329 2. 'F.' must always be exactly 'No right choice'.
2330 3. Place the correct answer randomly among 'A.'-'E.'; <=10% of items may have 'F' as the  

2331   correct answer.
2332 4. Distractors must be plausible and drawn from actual text/numbers in the OCR/captions.
2333 5. Make options mutually exclusive' no meta-options like "All of the above".
2334
2335 ---
2336
2337 ## EXPLANATION RULES
2338 - Provide a **step-by-step chain**: 'Step 1: ...', 'Step 2: ...', etc.
2339 - Explicitly cite which layouts were used as '[layout X]'.
2340 - Show all computations (e.g., "(132 - 95) / 95 = 0.389 = 38.9% [layout 4]").  

2341
2342 ---
2343
2344 ## OUTPUT FORMAT
2345 Return **only** the following JSON array - no extra text, no markdown outside the code  

2346 block, no commentary:
2347
2348
2349
2350
2351
2352
2353
2354
2355
2356
2357
2358
2359
2360
2361
2362
2363
2364
2365
2366
2367
2368
2369
2370
2371
2372
2373
2374
2375
2376
2377
2378
2379
2380
2381
2382
2383
2384
2385
2386
2387
2388
2389
2390
2391
2392
2393
2394
2395
2396
2397
2398
2399
2400
2401
2402
2403
2404
2405
2406
2407
2408
2409
2410
2411
2412
2413
2414
2415
2416
2417
2418
2419
2420
2421
2422
2423
2424
2425
2426
2427
2428
2429
2430
2431
2432
2433
2434
2435
2436
2437
2438
2439
2440
2441
2442
2443
2444
2445
2446
2447
2448
2449
2450
2451
2452
2453
2454
2455
2456
2457
2458
2459
2460
2461
2462
2463
2464
2465
2466
2467
2468
2469
2470
2471
2472
2473
2474
2475
2476
2477
2478
2479
2480
2481
2482
2483
2484
2485
2486
2487
2488
2489
2490
2491
2492
2493
2494
2495
2496
2497
2498
2499
2500
2501
2502
2503
2504
2505
2506
2507
2508
2509
2510
2511
2512
2513
2514
2515
2516
2517
2518
2519
2520
2521
2522
2523
2524
2525
2526
2527
2528
2529
2530
2531
2532
2533
2534
2535
2536
2537
2538
2539
2540
2541
2542
2543
2544
2545
2546
2547
2548
2549
2550
2551
2552
2553
2554
2555
2556
2557
2558
2559
2560
2561
2562
2563
2564
2565
2566
2567
2568
2569
2570
2571
2572
2573
2574
2575
2576
2577
2578
2579
2580
2581
2582
2583
2584
2585
2586
2587
2588
2589
2590
2591
2592
2593
2594
2595
2596
2597
2598
2599
2600
2601
2602
2603
2604
2605
2606
2607
2608
2609
2610
2611
2612
2613
2614
2615
2616
2617
2618
2619
2620
2621
2622
2623
2624
2625
2626
2627
2628
2629
2630
2631
2632
2633
2634
2635
2636
2637
2638
2639
2640
2641
2642
2643
2644
2645
2646
2647
2648
2649
2650
2651
2652
2653
2654
2655
2656
2657
2658
2659
2660
2661
2662
2663
2664
2665
2666
2667
2668
2669
2670
2671
2672
2673
2674
2675
2676
2677
2678
2679
2680
2681
2682
2683
2684
2685
2686
2687
2688
2689
2690
2691
2692
2693
2694
2695
2696
2697
2698
2699
2700
2701
2702
2703
2704
2705
2706
2707
2708
2709
2710
2711
2712
2713
2714
2715
2716
2717
2718
2719
2720
2721
2722
2723
2724
2725
2726
2727
2728
2729
2730
2731
2732
2733
2734
2735
2736
2737
2738
2739
2740
2741
2742
2743
2744
2745
2746
2747
2748
2749
2750
2751
2752
2753
2754
2755
2756
2757
2758
2759
2760
2761
2762
2763
2764
2765
2766
2767
2768
2769
2770
2771
2772
2773
2774
2775
2776
2777
2778
2779
2780
2781
2782
2783
2784
2785
2786
2787
2788
2789
2790
2791
2792
2793
2794
2795
2796
2797
2798
2799
2800
2801
2802
2803
2804
2805
2806
2807
2808
2809
2810
2811
2812
2813
2814
2815
2816
2817
2818
2819
2820
2821
2822
2823
2824
2825
2826
2827
2828
2829
2830
2831
2832
2833
2834
2835
2836
2837
2838
2839
2840
2841
2842
2843
2844
2845
2846
2847
2848
2849
2850
2851
2852
2853
2854
2855
2856
2857
2858
2859
2860
2861
2862
2863
2864
2865
2866
2867
2868
2869
2870
2871
2872
2873
2874
2875
2876
2877
2878
2879
2880
2881
2882
2883
2884
2885
2886
2887
2888
2889
2890
2891
2892
2893
2894
2895
2896
2897
2898
2899
2900
2901
2902
2903
2904
2905
2906
2907
2908
2909
2910
2911
2912
2913
2914
2915
2916
2917
2918
2919
2920
2921
2922
2923
2924
2925
2926
2927
2928
2929
2930
2931
2932
2933
2934
2935
2936
2937
2938
2939
2940
2941
2942
2943
2944
2945
2946
2947
2948
2949
2950
2951
2952
2953
2954
2955
2956
2957
2958
2959
2960
2961
2962
2963
2964
2965
2966
2967
2968
2969
2970
2971
2972
2973
2974
2975
2976
2977
2978
2979
2980
2981
2982
2983
2984
2985
2986
2987
2988
2989
2990
2991
2992
2993
2994
2995
2996
2997
2998
2999
3000
3001
3002
3003
3004
3005
3006
3007
3008
3009
3010
3011
3012
3013
3014
3015
3016
3017
3018
3019
3020
3021
3022
3023
3024
3025
3026
3027
3028
3029
3030
3031
3032
3033
3034
3035
3036
3037
3038
3039
3040
3041
3042
3043
3044
3045
3046
3047
3048
3049
3050
3051
3052
3053
3054
3055
3056
3057
3058
3059
3060
3061
3062
3063
3064
3065
3066
3067
3068
3069
3070
3071
3072
3073
3074
3075
3076
3077
3078
3079
3080
3081
3082
3083
3084
3085
3086
3087
3088
3089
3090
3091
3092
3093
3094
3095
3096
3097
3098
3099
3100
3101
3102
3103
3104
3105
3106
3107
3108
3109
3110
3111
3112
3113
3114
3115
3116
3117
3118
3119
3120
3121
3122
3123
3124
3125
3126
3127
3128
3129
3130
3131
3132
3133
3134
3135
3136
3137
3138
3139
3140
3141
3142
3143
3144
3145
3146
3147
3148
3149
3150
3151
3152
3153
3154
3155
3156
3157
3158
3159
3160
3161
3162
3163
3164
3165
3166
3167
3168
3169
3170
3171
3172
3173
3174
3175
3176
3177
3178
3179
3180
3181
3182
3183
3184
3185
3186
3187
3188
3189
3190
3191
3192
3193
3194
3195
3196
3197
3198
3199
3200
3201
3202
3203
3204
3205
3206
3207
3208
3209
3210
3211
3212
3213
3214
3215
3216
3217
3218
3219
3220
3221

```

```

2322
2323     ````json
2324     [
2325         {
2326             "question": "...",
2327             "options": "A. ...\\nB. ...\\nC. ...\\nD. ...\\nE. ...\\nF. No right choice",
2328             "answer": "C",
2329             "explanation": "Step 1: ... [layout 2]\\nStep 2: ... [layout 5]\\nStep 3: ..."
2330         },
2331         ...
2332     ]
2333     ````
```

For map images, we use the following prompt for GPT-5 (OpenAI, 2025a) to automatically generate QA instances.

```

2334
2335     You are an expert evaluation-item author who designs rigorous **multi-hop visual-reasoning
2336     ** questions to benchmark "think-with-images" abilities on **maps** (bus/metro networks,
2337     terminals, malls, festivals, parks, etc.). Items should be challenging enough that today's
2338     strongest MLLMs achieve **<= 50%** accuracy.
2339
2340     You will receive:
2341
2342     ### INPUTS
2343     1. **GLOBAL_OCR** - OCR or caption text describing the entire map.
2344         {GLOBAL_OCR}
2345     2. **GLOBAL_CAPTION** - caption text describing the entire map.
2346         {GLOBAL_CAPTION}
2347     3. **LAYOUTS** - a list of cropped map regions. Each layout contains:
2348         - 'layout_id' - unique numeric ID (for your internal reference only).
2349         - 'caption_or_ocr' - OCR or descriptive caption of the cropped region.
2350             {LAYOUTS}
2351
2352     > **Hard requirement:** In the **question** and **options**, you must use only natural
2353     labels/text found in 'GLOBAL_OCR' or 'GLOBAL_CAPTION' or 'caption_or_ocr'.
2354     > Do **not** mention 'layout_id', 'region', 'crop', 'box', 'panel', or similar. Layouts are
2355     **reference-only** for your reasoning; you may cite them in the **explanation**, but never
2356     in the question or options.
2357
2358     ---
2359
2360     ## TASK
2361     Generate **3-5 independent multiple-choice questions**.
2362     Each question must require **>=2 distinct reasoning hops** that combine information across
2363     different layouts or between global and local OCR. All facts must be image-grounded.
2364
2365     ---
2366
2367     ## 1) QUESTION-DESIGN RULES
2368     1. **Multi-hop reasoning (mandatory).** Examples of valid hops:
2369         - Legend <-> line color <-> stop/zone.
2370         - Grid index <-> label <-> adjacency.
2371         - Level/floor marker <-> facility <-> inset.
2372         - Route <-> timetable <-> destination.
2373         - Symbol <-> restriction <-> path feasibility.
2374         - Distance/scale <-> number of segments <-> travel time.
2375
2376     2. **Image/OCR grounded only.** Do not use external/world knowledge.
2377
2378     3. **Diversity.** Vary question styles (routing, conditional reachability, transfer logic,
2379     adjacency/containment, count/compare, scale-based).
2380
2381     4. **Difficulty target.** Avoid "at-a-glance" items. Require cross-checking, counting, or
2382     lightweight calculation.
2383
2384     5. **Label fidelity.** Copy map labels exactly (case, spelling, diacritics).
2385
2386     6. **Uniqueness.** Ensure exactly **one correct answer** among A-E, unless F ("No right
2387     choice") is deliberately correct.
2388
2389     7. **Units & scale.** If computing length/time/segments, use the map's own scales, symbols,
2390     or counts.
2391
2392     ---
2393
2394     ## 2) ANSWER-OPTION RULES
2395     1. Provide **exactly six** options labeled 'A.' ... 'F.'.
```

```

2376 2. 'F.' must always be 'No right choice'.
2377 3. Normally, the correct answer is among A-E; only rarely (<10%) should 'F' be correct.
2378 4. Distractors must be plausible, drawn from real map text/numbers, and mutually exclusive.
2379 5. No meta-options ("All of the above").
2380 ---
2381 ## 3) EXPLANATION RULES
2382 - Provide a **step-by-step reasoning chain**.
2383 - Explicitly cite layouts used as '[layout X]'.
2384 - Make hops and computations explicit (e.g., "Count 5 stops along Red Line [layout 3] and
2385 compare to 4 stops in Zone B [layout 5]").  

2386 ---
2387 ## 4) OUTPUT FORMAT
2388 Return **only** the following JSON array-no extra commentary or markdown:  

2389   

2390   

2391   

2392   

2393   

2394   

2395   

2396   

2397

```

H.3 PROMPTS FOR EVALUATION

For the evaluation of API models, we adopt the commonly used thinking prompt as follows.

```

2401 A conversation between User and Assistant. The user asks a question, and the Assistant
2402 solves it.
2403 The assistant first thinks about the reasoning process in the mind and then provides the
2404 user with the answer.
2405 The reasoning process and answer are enclosed within <think> </think> and <answer> </answer>
2406 tags, respectively,
2407 And the final answer letter is enclosed within \boxed{{option letter}}.
2408 i.e., <think> reasoning process here </think><answer> answer here \boxed{{option letter}}
2409 </answer>.

```

I PROMPTS FOR INSIGHT-O3

I.1 vREASONER PROMPTS

We use the following prompts for vReasoner during training.

```

2410 [SYSTEM]
2411 You are a visual assistant. Your goal is to answer a question based on an image.
2412
2413 First, think step by step to identify which visual facts you need from the image to answer
2414 the question. If the visual information is insufficient or unclear, call the visual search
2415 tool by providing a concise region description:
2416 <tool_call>region_description={...}</tool_call>
2417
2418 The tool will search the image and return a cropped view of the target region. You may
2419 repeat this process until you have enough evidence to answer confidently. The tool is not
2420 always precise -- evaluate its output critically. If it looks incorrect or off-target,
2421 refine your description and try again.
2422
2423 Region description guidance:
2424 - Use concise, visually grounded targets (e.g., a chart, an object, a text block, a
2425 distinct area)
2426 - Optionally include approximate location (e.g., top-left, bottom-right, center)
2427 - Avoid non-visual or ordinal references (e.g., "the third largest bar", "the second row's
2428 number")
2429 - Describe only one region per tool call; do not request multiple regions in a single
description

```

```

2430
2431     Output format:
2432     - Put your reasoning process inside <think>...</think>.
2433     - Immediately after </think>, output your assessment of the most recent tool result (if any)
2434     ) formatted as <tool_feedback>helpful/unhelpful</tool_feedback>.
2435     This should indicate whether the result returned by the previous tool call is relevant to
2436     your prior region description and helpful to answering the question. If it misses the
2437     key information you are looking for, it is unhelpful. If no previous tool result exists (e.g.,
2438     the first turn), output <tool_feedback>NA</tool_feedback>.
2439     - Immediately after </tool_feedback>, do exactly one of:
2440         1) Call the tool; or
2441         2) Provide the final answer (no tool call) -- include the result in \boxed{...}. Do not
2442         mix tool calls and answers in the same turn.
2443     - If you need to call the tool, provide the region description using the exact format <
2444     tool_call>region_description={...}</tool_call>.
2445     You must strictly follow the output format, otherwise your answer will be judged as wrong.
2446
2447     A multi-turn format example:
2448     Assistant:
2449     <think>{your step-by-step analysis; decide if more detail is needed}</think>
2450     <tool_feedback>NA</tool_feedback>
2451     <tool_call>region_description={concise, visually grounded target (optionally with location)}</tool_call>
2452
2453     User:
2454     [Zoomed-in image + guidance (e.g., "Based on your description, here is the zoomed-in image.
2455     Please continue your analysis; you may call the tool again or provide your final answer if
2456     sufficient.")]
```

Assistant:

```

2457     <think>{updated analysis based on the zoomed-in view; decide whether to refine or answer}</think>
2458     <tool_feedback>unhelpful</tool_feedback>
2459     <tool_call>region_description={next concise target (optionally with location)}</tool_call>
2460
2461     (Repeat the User -> Assistant pattern as needed until enough evidence is gathered.)
```

Assistant (final turn):

```

2462     <think>{final reasoning; explain why the available visual evidence is sufficient}</think>
2463     <tool_feedback>helpful</tool_feedback>
2464     Answer: \boxed{...}
```

[USER]

[question]<image>

[ASSISTANT]

[USER]

Based on your description, here is the zoomed-in image.

Please continue your analysis. After the analysis, state your assessment of the previous tool result using <tool_feedback>helpful/unhelpful</tool_feedback>, then do one of the following:

- Call the tool again if you believe more visual detail is needed; or
- Provide your final answer if the current information is sufficient.

<image>

[ASSISTANT]

[USER]

Based on your description, here is the zoomed-in image.

You have reached the limit for using the visual tool and cannot call it again.

In this turn, after reasoning step by step, output your assessment of the previous tool result using exactly <tool_feedback>helpful/unhelpful</tool_feedback>, and then, based on the available information, provide your final answer using the required format.

<image>

[ASSISTANT]

In case that vSearcher is unable to find a region that matches the region description provided by vReasoner, we use the following user prompt to notify vReasoner.

2484

[USER]
The visual searcher could not locate the requested target in the image based on your description.

2487

Please adjust or refine your region description (for example, refer to a larger, clearly visible area) and continue your analysis. Think first, then state your assessment of the previous tool result using <tool_feedback>helpful/unhelpful</tool_feedback>. Finally, do exactly one of the following:

- Call the tool again with a revised description; or
- Provide your final answer if the current information is sufficient.

2490

2491

2492

2493
2494
2495

Occasionally, vReasoner may fail to follow the format instructions. When this happens, we use the following user prompt to ask vReasoner to generate a new response:

2496

[USER]
In your previous response, neither a tool call nor a final boxed answer was detected, or you didn't output your assessment of the previous tool result in the correct format.

2498

Think first, and then include your assessment of the previous tool result using exactly <tool_feedback>helpful/unhelpful</tool_feedback> (or <tool_feedback>NA</tool_feedback> if there is no previous result). Finally, do exactly one of the following:

- If you still need more visual detail, call the tool using the exact format:
<tool_call>region_description={...}</tool_call>
- Otherwise, provide the final answer now and include the result in \boxed{...}.

2503

2504

2505

During inference, we do not ask vReasoner to provide any feedback to the tool. The prompts are slightly simplified as follows:

2507

2508

[SYSTEM]
You are a visual assistant. Your goal is to answer a question based on an image.

2509

First, think step by step to identify which visual facts you need from the image to answer the question. If the visual information is insufficient or unclear, call the visual search tool by providing a concise region description:
<tool_call> region_description={...} </tool_call>

2512

The tool will search the image and return a cropped view of the target region. You may repeat this process until you have enough evidence to answer confidently. The tool is not always precise -- evaluate its output critically. If it looks incorrect or off-target, refine your description and try again.

2513

Region description guidance:

- Use concise, visually grounded targets (e.g., a chart, an object, a text block, a distinct area)
- Optionally include approximate location (e.g., top-left, bottom-right, center)
- Avoid non-visual or ordinal references (e.g., "the third largest bar", "the second row's number")
- Describe only one region per tool call; do not request multiple regions in a single description

2522

Output format:

- Put your reasoning process inside <think>...</think>.
- When you need to call the tool, you need to provide the region description using the format <tool_call>region_description={...}</tool_call>.
- Immediately after each </think>, do exactly one of:
 - 1) Call the tool; or
 - 2) Provide the final answer (no tool call) -- include the result in \boxed{...}. Do not mix tool calls and answers in the same turn.

2528

You must strictly follow the output format, otherwise your answer will be judged as wrong.

2529

A multi-turn format example:

Assistant:

<think>{your step-by-step analysis; decide if more detail is needed}</think>
<tool_call> region_description={concise, visually grounded target (optionally with location)} </tool_call>

2533

User:

[Zoomed-in image + guidance (e.g., "Based on your description, here is the zoomed-in image. Please continue your analysis; you may call the tool again or provide your final answer if sufficient.")]

2536

Assistant:

2537

```

2538 <think>{updated analysis based on the zoomed-in view; decide whether to refine or answer}</
2539 think>
2540 <tool_call> region_description={next concise target (optionally with location)} </tool_call>
2541 >
2542 (Repeat the User -> Assistant pattern as needed until enough evidence is gathered.)
2543 Assistant (final turn):
2544 <think>{final reasoning; explain why the available visual evidence is sufficient}</think>
2545 Answer: \boxed{...}
2546 [USER]
2547 {question}<image>
2548 [ASSISTANT]
2549 ...
2550 [USER]
2551 Based on your description, here is the zoomed-in image.
2552 Please continue your analysis. You may:
2553 - Call the tool again if you believe more visual detail is needed; or
2554 - Provide your final answer if the current information is sufficient.
2555 <image>
2556 [ASSISTANT]
2557 ...
2558 [USER]
2559 Based on your description, here is the zoomed-in image.
2560 You have reached the limit for using the visual tool and cannot call it again.
2561 In this turn, based on the available information, provide your final answer using the
2562 required format.
2563 <image>
2564 [ASSISTANT]
2565 ...
2566

```

When vSearcher can't find the target region, we use the following user prompt to notify vReasoner:

```

2567 [USER]
2568 The visual searcher could not locate the requested target in the image based on your
2569 description.
2570 Please adjust or refine your region description (for example, refer to a larger, clearly
2571 visible area) and continue your analysis. You may:
2572 - Call the tool again with a revised description; or
2573 - Provide your final answer if the current information is sufficient.

```

When vReasoner fails to follow the format instruction described in the system prompt, we the following user prompt to ask vReasoner to generate a new response:

```

2574 [USER]
2575 In your previous response, neither a tool call nor a final boxed answer was detected.
2576 Please do exactly one of the following:
2577 - If you still need more visual detail, call the tool using the exact format:
2578   <tool_call>region_description={...}</tool_call>
2579 - Otherwise, provide the final answer now and include the result in \boxed{...}.
2580
2581
2582
2583

```

I.2 VSEARCHER PROMPTS

We use the following prompts for vSearcher during both training and evaluation after training. The prompts are adapted from DeepEyes (Zheng et al., 2025). For the last turn, we notify vSearcher in the user prompt that it has reached tool call limit.

```

2589 [SYSTEM]
2590 You are a helpful assistant.
2591

```

```

2592 # Tools
2593 You may call one or more functions to assist with the user query.
2594 You are provided with function signatures within <tools></tools> XML tags:
2595 <tools>
2596 {"type":"function","function":{"name":"image_zoom_in_tool","description":"Zoom in on a
2597 specific region of an image by cropping it based on a bounding box (bbox) and an optional
2598 object label.,"parameters":{"type":"object","properties":{"bbox_2d":{"type":"array","items
2599 ":"{"type":"number"},"minItems":4,"maxItems":4,"description":"The bounding box of the region
2600 to zoom in, as [x1, y1, x2, y2], where (x1, y1) is the top-left corner and (x2, y2) is the
2601 bottom-right corner."},"label":{"type":"string","description":"The name or label of the
2602 object in the specified bounding box (optional)."}},"required":["bbox"]}}
2603 </tools>
2604
2605 # How to call a tool
2606 Return a json object with function name and arguments within <tool_call></tool_call> XML
2607 tags:
2608 <tool_call>
2609 {"name": <function-name>, "arguments": <args-json-object>}
2610 </tool_call>
2611
2612 Example:
2613 <tool_call>
2614 {"name": "image_zoom_in_tool", "arguments": {"bbox_2d": [10, 20, 100, 200], "label": "the
2615 apple on the desk"}}
2616 </tool_call>
2617
2618 [USER]
2619 <image>
2620 Locate {target}.
2621 Think first, call image_zoom_in_tool if needed, then answer with the bbox coordinates in [x1,
2622 y1, x2, y2] format (or [0, 0, 0, 0] if you can't locate it). Format strictly as: <
2623 think>...</think> <tool_call>...</tool_call> (if tools needed) <answer>[x1, y1, x2, y2]</
2624 answer> (otherwise)
2625
2626 [ASSISTANT]
2627 ...
2628
2629 [USER]
2630 <tool_response><image></tool_response>
2631 Think first, call image_zoom_in_tool if needed, then answer with the bbox coordinates in [x1,
2632 y1, x2, y2] format (or [0, 0, 0, 0] if you can't locate it). Format strictly as: <
2633 think>...</think> <tool_call>...</tool_call> (if tools needed) <answer>[x1, y1, x2, y2]</
2634 answer> (otherwise)
2635
2636 [ASSISTANT]
2637 ...
2638
2639
2640
2641
2642
2643
2644
2645

```

Without RL, Qwen2.5-VL-7B has difficulty following the instructions given in the above prompts. So, for evaluating vReasoner + Qwen2.5-VL-7B, we use the following simple prompt:

```

2634 [SYSTEM]
2635 You are a helpful assistant.
2636
2637 [USER]
2638 Given an image and a region description, locate the region that best matches the
2639 description and output its bounding box coordinates as [x_min, y_min, x_max, y_max].
2640
2641 If the target cannot be found, output [0, 0, 0, 0].
2642
2643 Region description:
2644 {target}
2645
2646 Now, output the coordinates in format [x_min, y_min, x_max, y_max]:
2647 <image>
2648
2649 [ASSISTANT]
2650 ...

```

2646

2647

2648

2649

I.3 PROMPTS FOR ANSWER VERIFICATION

2650

2651 For answer verification, we use GPT-5-nano (OpenAI, 2025a) and feed it with the following prompt.

2652

2653

2654

2655

2656

2657

2658

2659

2660

2661

2662

2663

2664

You are given an image-based question, the ground truth (GT) answer, and a model’s answer.

Compare the model’s answer with the GT answer:

- If the model’s answer matches the GT answer visually or semantically, reply with <correct>.
- If it doesn’t match, or if uncertain, reply with <wrong>.

Only reply with <correct> or <wrong>, no explanations.

Question: {question}

GT Answer: {gt_answer}

Model Answer: {model_answer}

J EVALUATION BENCHMARKS

J.1 NATURAL-IMAGE BENCHMARKS

- **V^{*}-Bench** (Wu & Xie, 2024) is designed to test a model’s ability to attend to high-resolution, detail-rich images. V^{*}-Bench consists of 191 challenging natural images (sourced from the SA-1B Segment Anything dataset (Kirillov et al., 2023)) and focuses on two fine-grained visual tasks: attribute recognition (identifying specific object attributes like color or material) and spatial relationship reasoning (determining the relative positions of objects). By requiring accurate visual grounding of small details, V^{*}-Bench exposes the limitations of models that rely on coarse image understanding.

- **Tree-Bench** (Wang et al., 2025a), like V^{*}-Bench, uses high-quality, object-dense natural images (drawn from the SA-1B dataset) to evaluate fine-grained visual reasoning. However, Tree-Bench places additional emphasis on traceable evidence and complex reasoning. Each of its 405 visual question-answer pairs is annotated with bounding-box evidence for the correct answer, and many questions require second-order reasoning about object interactions or spatial hierarchies rather than simple identification.

- **VisualProbe** (Lai et al., 2025) pushes visual reasoning to an even harder regime. It features high-resolution images with very small target objects and many distractors, making it “super challenging” and necessitating iterative, trial-and-error search by the model. VisualProbe is organized into easy, medium, and hard subsets; VisualProbe-Hard denotes the toughest set of questions (106 in total) that often cannot be solved in a single glance. Compared to V^{*}-Bench and Tree-Bench, VisualProbe-Hard scenarios demand an active visual search strategy: the model may need to zoom in on different regions or sequentially explore the image to find relevant details.

J.2 MIXED BENCHMARKS

- **HR-Bench** (Wang et al., 2025f) is a benchmark deliberately designed to evaluate models on ultra high-resolution images (up to 4K-8K pixels). It addresses a key limitation of prior multimodal tests (which max out at \sim 2K resolution) by presenting tasks that cannot be solved with down-sampled images. HR-Bench is split into two sub-task categories: (1) Fine-grained Single-instance Perception (FSP), with tasks like identifying detailed attributes of a single object, reading text via OCR, or responding to visual prompts on an image; and (2) Fine-grained Cross-instance Perception (FCP), which includes more complex multi-object challenges such as analyzing maps, interpreting charts/graphs, and assessing spatial relationships among multiple items. Each sub-task contains 100 queries on 8K-resolution images (with a downsampled 4K version also provided for efficiency).

2700
2701
2702 Table 7: Comparison of O3-BENCH and related benchmarks.
2703
2704
2705
2706

Benchmark	# of QAs	Image domains	Layout/target boxes	Detailed explanations	Multi-hop	Avg. resolution
V*-Bench	191	natural (100%)	✓	✗	✗	2246×1583
Tree-Bench	405	natural (100%)	✗	✗	✗	2152×1615
VisualProbe _{Hard}	106	natural (100%)	✗	✗	✗	4944×3980
HR-Bench _{4K}	200*	natural (89%), chart (5%), map (6%)	✗	✗	✗	4024×3503
MME-RealWorld	~29K	natural (>60%), chart (25%), map (6%), etc.	✗	✗	✗	2708×1844
O3-Bench	318	chart (43%), map (57%)	✓	✓	✓	4602×3967

2707
2708
2709
2710
2711
2712
2713
2714 * Roughly 200 distinct QA pairs. The original paper reported 800 but most are the same questions with scrambled options.
2715
2716
2717
2718
2719
2720
2721
2722
2723
2724
2725
2726
2727
2728
2729
2730
2731
2732
2733
2734
2735
2736
2737
2738
2739
2740
2741
2742
2743
2744
2745
2746
2747
2748
2749
2750
2751
2752
2753

Table 8: Comparison of O3-BENCH and related benchmarks on chart & map.

Benchmark	Avg. resolution	Avg. acc. of GPT-5-mini	Avg. # of vSearch steps
HR-Bench _{4K}	4032×2509	79.6	2.3
MME-RealWorld	1875×1269	83.8*	1.0
O3-Bench	4602×3967	38.1	2.9

* Based on 500 random samples.

- **MME-RealWorld** (Zhang et al., 2024b) is a large-scale, comprehensive benchmark that evaluates models across a wide spectrum of real-world visual tasks. It comprises 13,366 high-quality images (average $\sim 2000 \times 1500$ resolution) and 29,429 QA pairs, spanning 43 distinct task types grouped into five real-world scenarios, curated from various datasets (Agustsson & Timofte, 2017; Liu et al., 2020; Zhang et al., 2021; Yang et al., 2023; Li et al., 2022; Sun et al., 2022; Sachdeva et al., 2024; Zhu et al., 2021; Jia et al., 2021). These scenarios cover diverse applications such as autonomous driving (e.g., interpreting traffic scenes), video surveillance (e.g., counting vehicles in an overhead street video), remote sensing (e.g., identifying and counting tiny objects in satellite maps), sports and entertainment (e.g., reading a scoreboard in a broadcast image), and others. MME-RealWorld is notable as the largest fully human-annotated multimodal benchmark to date. Given the benchmark’s scale, we employ the official MME-RealWorld lite version³ for efficiency, which uses a subset of 50 samples per task to speed up evaluation without significantly altering the task distribution.

J.3 COMPARISON OF O3-BENCH AND RELATED BENCHMARKS

In Table 7 and Table 8, we compare O3-BENCH with related benchmarks and highlight their key differences. Compared with the most closely related MME-RealWorld, we note that on the overlapping domains (i.e. chart & map): (i) the average image resolution of O3-BENCH is *significantly higher* (4602×3967 of ours *vs* 1875×1269 of MME-RealWorld); (ii) the average accuracy of GPT-5-mini on O3-BENCH is much lower (38.1% of ours *vs* 83.8% of MME-RealWorld); and (iii) the average number of visual search steps produced by InSight-o3 for O3-BENCH is 2.9× that of MME-RealWorld. In addition, O3-BENCH provides layout boxes and detailed explanations for each QA pair, while most of the benchmarks do not. The explanations can help the community easily verify the correctness of the answers. These differences show that O3-BENCH is of exceptional quality and much harder to solve than the other related benchmarks.

Apart from quality, the scale of O3-BENCH is on par with most of the fine-grained perception multimodal understanding benchmarks, e.g., V*-Bench (191), Tree-Bench (405), VisualProbe-Hard

³<https://huggingface.co/datasets/yifanzhang114/MME-RealWorld-Lite>

(106), HR-Bench-4K (200*), and commonly-used benchmarks in other multimodal research areas; to list a few: Math: MathVision test-mini (304) (Wang et al., 2024), MathVista test-mini (1K) (Lu et al., 2023); VQA: RealWorldQA⁴ (765); Embodiment/Spatial Understanding: ERQA (400) (Team et al., 2025a), RefSpatial-Bench (277) (Zhou et al., 2025); Agent: MIA Bench (400) (Qian et al., 2024), OSWorld (389) (Xie et al., 2024), AndroidWorld (116) (Rawles et al., 2024); Fine-grained Perception: V*-Bench. These benchmarks were used to evaluate the performance of Qwen3-VL⁵. As with O3-BENCH, these benchmarks are relatively small mainly because of the difficulty in data collection. Nevertheless, they have served the timely purpose of evaluating frontier models in the respective areas which are fast developing.

O3-BENCH only focuses on composite charts and digital maps for two main reasons. First, they are *representative* of most use cases of thinking with images in the digital domain (as opposed to the natural domain). More specifically, composite charts represent *structured* images (with clear delineations between different layout regions) and often require more *abstract* reasoning (e.g., computing the difference of two quantities). On the other hand, digital maps represent images with less structure and more *organic* layouts. They usually require more *visual* reasoning (e.g., finding the shortest route from location A to B). Together, we argue that O3-BENCH is generally sufficient for evaluating the thinking-with-image capability of current multimodal models in the digital domain. As for the natural domain, there are already a number of high-quality benchmarks for thinking with natural images (some are listed in Table 7). O3-BENCH precisely fills the gap of existing benchmarks while striking a balance between evaluation efficiency and generality.

2773

2774

2775

2776

2777

2778

2779

2780

2781

2782

2783

2784

2785

2786

2787

2788

2789

2790

2791

2792

2793

2794

2795

2796

2797

2798

2799

2800

2801

2802

2803

2804

2805

2806

⁴<https://huggingface.co/datasets/xai-org/RealworldQA>

⁵<https://github.com/QwenLM/Qwen3-VL>